RMP Colloquia

Solar neutrino experiments: results and implications

Till A. Kirsten

Max-Planck-Institut für Kernphysik Heidelberg, P.O. Box 103 980, D-69029 Heidelberg, Germany

The neutrinos that are produced in the solar fusion reaction chains reflect the conditions in the stellar interior. If the model predictions for the expected neutrino fluxes are firm, then the solar neutrino experiments can also test neutrino properties during propagation along the 1.5×10^8 kilometer ''baseline'' between ''source'' and detector. So far, results have been acquired with five solar neutrino detectors: Homestake, Kamiokande, Superkamiokande, Gallex, and Sage. Taking all of the experimental data together, it appears that the abundant pp neutrinos are present, the moderately abundant ^{7}Be neutrinos are strongly or totally suppressed, and the rare ^{8}B neutrinos are partially reduced, by a factor of about three. This outcome cannot be explained by modifications of the stellar model but it is consistent with the hypothesis of neutrino flavor oscillations. Such oscillations could occur on the way between the solar core and the detector. In such a scenario, a nonvanishing neutrino rest mass would follow. The evidence is summarized here, and the outlook as regards anticipated future experiments is briefly discussed.
[S0034-6861(99)00504-8]

CONTENTS

I. Introduction 1213
II. Expected Solar Neutrino Fluxes 1214
A. Solar neutrino generation 1214
B. Neutrino mass mediated propagation phenomena 1215
1. Time variations 1216
III. Detection Principles 1216
A. Characteristic features of solar neutrino experiments 1216
B. Detector types 1217
1. Radiochemical detectors 1217
2. Real-time detectors 1217
3. Cryogenic and bolometric detectors 1218
4. Geochemical solar neutrino detectors 1218
IV. Results from Solar Neutrino Experiments 1218
A. Homestake chlorine detector, based on $^{37}\mathrm{Cl}(\nu_e,e^-)^{37}\mathrm{Ar}$ 1218
B. Kamiokande Čerenkov detector, based on $e^-(\nu_x,\nu_x)e^-$ 1220
C. Superkamiokande detector, based on $e^-(\nu_x,\nu_x)e^-$ 1221
D. Gallex gallium chloride detector, based on $^{71}\mathrm{Ga}(\nu_e,e^-)^{71}\mathrm{Ge}$ 1221
1. Verification of performance and results 1222
E. Sage gallium metal detector, based on $^{71}\mathrm{Ga}(\nu_e,e^-)^{71}\mathrm{Ge}$ 1223
V. Implications 1224
A. Solar neutrino problems 1224
B. Neutrino oscillations 1226
C. Neutrino mass and new physics 1226
1. How compelling is the evidence for new physics from solar neutrinos? 1227
VI. Outlook 1227
A. Near future 1227
B. Far future 1228
Acknowledgments 1229
List of Symbols 1229
References 1230

I. INTRODUCTION

Weak interactions are involved at various stages of the fusion reaction network that operates in the solar interior. As a result, neutrinos are produced in the solar core when hydrogen is fused to form helium. The neutrinos leave the solar core virtually unhindered, distinct from photons or any other radiation. After penetration of ≈700 000 km of solar matter at decreasing density and after subsequent travel through interplanetary space for 1.5×10^8 kilometers (1 AU), the neutrinos can reach a detector on Earth, either from the front or from the back, within ≈8 minutes, or practically in real time. If detected, the neutrinos can serve as messenger particles about the present state of the solar interior and the reactions occurring therein. This allows experimental tests of theoretical solar models. Such knowledge is fundamental for astrophysics and for models of stellar structure in general since the Sun is a standard main sequence star.

From the particle physics point of view, the Sun is a very strong low-energy neutrino source at a great distance. It is well suited to test the properties of a neutrino ''beam'' while it propagates in a number of distinct environments. First, the very dense medium in which the neutrinos are formed, second, the region of decreasing electron densities that occur as the neutrinos travel to the solar surface, third, the vacuum at space, and finally, the interior of the Earth if the detector is at the night side. These are ideal conditions for a ''long-baseline experiment'' to search for neutrino flavor transmutations and thus for manifestations of a nonvanishing neutrino rest mass. For this application, the source strength (the neutrino source function) must be reliably known, and the detector must be flavor specific. Solar neutrinos are generated as electron neutrinos. A detector tuned to ν_e would register a flux-deficit relative to expectation if

transformations into muon- or tau-neutrinos (ν_μ, ν_τ) would occur (i.e., a "disappearance experiment").

Experimentally, solar neutrino detection is difficult due to the very low rates for the interaction of low energy neutrinos with matter. The penetrating power of neutrinos, so beneficial for unhindered movement through the Sun, is less appreciated once they cross a detector. Huge target sizes, extreme (single event) detection sensitivities and rigorous background reduction are therefore characteristic for solar neutrino experiments.

The plan of this article is as follows. In Sec. II.A, we outline the reactions that produce neutrinos and the predictions for the fluxes that result from the standard solar model (SSM). The general concept of neutrino oscillations as a potential reason for neutrino flux reductions is introduced in Sec. II.B. Section III addresses the general methods to detect solar neutrinos. Common features are described in Sec. III.A, detector types in Sec. III.B. In Sec. IV, we discuss the five operating (or completed) experiments for which solar neutrino results are published: Sec. IV.A, the Homestake Chlorine detector; Sec. IV.B, the Kamiokande and Sec. IV.C, the Superkamiokande Čerenkov detectors; Sec. IV.D, the Gallex gallium chloride detector; and Sec. IV.E, the Sage gallium metal detector. In Sec. V, we present the implications from an analysis of all available solar neutrino data. The pattern that has emerged from the data is described in terms of "solar neutrino problems" (Sec. V.A). The probable solution of these problems is neutrino oscillations (Sec. V.B). In Sec. V.C, we outline the neutrino masses that result from this interpretation. In Sec. VI, we describe upcoming experiments; in Sec. VI.A, we describe those that are already under construction and that are expected very soon to yield results and answers to specific open questions; and in Sec. VI.B, we enumerate those that are planned or projected to come into operation in the future. An Appendix contains a glossary of the less common symbols and abbreviations that are used in this article.

II. EXPECTED SOLAR NEUTRINO FLUXES

A. Solar neutrino generation

The major ingredients for a quantitative description of the state of the stellar interior are (1) hydrostatic equilibrium (stationary), (2) equation of state (ideal gas), (3) thermal equilibrium (radiation-dominated), and (4) energy production (by hydrogen fusion; also leading to neutrino production).

The major input data are the solar mass, radius, luminosity, age, chemical composition, *S*-factors (nuclear reaction cross sections), and radiative opacities. The foundations for the solar models were set by Eddington, Critchfield, Bethe, v. Weizsäcker, Gamov, Vogt, and Fowler. During the last 30 years, modern quantitative models have been continuously elaborated and improved by J. N. Bahcall (Bahcall *et al.*, 1969; Bahcall and Ulrich, 1988; Bahcall, 1989; Bahcall and Pinsonneault, 1992; Bahcall and Pinsonneault, 1995; Bahcall *et al.*, 1998a). For each such solar model, the expected neutrino fluxes have also been derived. Independent calculations confirm the respective results as long as the same input parameters are used (Turck-Chieze and Lopes, 1993; Profitt, 1994; Castellani *et al.*, 1997; Morel *et al.*, 1997), taking exception for the ^{8}B-neutrino flux deduced by Dar and Shaviv (1996).

Specific new models usually add more detail concerning various physical aspects, such as screening effects, diffusion, composition, or others. Such refinements may or may not apply, but the models still stick to the basic principles. Similarly, differences exist between the various parameters that are used, especially as regards the radiative opacities. In any case, the freedom to speculate on "nonstandard" models in order to "tailor" the neutrino fluxes for better agreement with observation is now severely restricted. This is because of the remarkable agreement of the standard solar model with the solar density profiles that are experimentally obtained from helioseismological observations (Basu *et al.*, 1997; see also Bahcall *et al.*, 1997; Paterno, 1997).

The net generation of fusion energy is reflected in the sum equation

$$4\mathrm{H}^+ + 2e^- \rightarrow {}^4\mathrm{He}^{++} + 2\nu_e + 26.73 \text{ MeV},$$
$$\langle E(2\nu_e)\rangle = 0.59 \text{ MeV}. \quad (1)$$

Along the way, arising from "cycles," the following kinds of neutrino emissions are expected:
"PP I"-cycle:
pp neutrinos from

$$p + p \rightarrow d + e^+ + \nu_e \quad (99.77\%) \quad (2)$$

and pep-neutrinos from

$$p + p + e^- \rightarrow d + \nu_e \quad (0.23\%) \quad (3)$$

"PP II"-cycle:
^{7}Be neutrinos from

$${}^7\mathrm{Be} + e^- \rightarrow {}^7\mathrm{Li} + \nu_e, \quad (4)$$

where ^{7}Be stems from

$${}^3\mathrm{He} + {}^4\mathrm{He} \rightarrow {}^7\mathrm{Be} + \gamma \quad (15\%). \quad (5)$$

The production of ^{7}Be is in competition with the reaction

$${}^3\mathrm{He} + {}^3\mathrm{He} \rightarrow {}^4\mathrm{He} + 2\,{}^1\mathrm{H} \quad (85\%), \quad (6)$$

in which no neutrinos are produced.
"PP III"-cycle:
^{8}B neutrinos from

$${}^8\mathrm{B} \rightarrow {}^8\mathrm{Be} + e^+ + \nu_e, \quad (7)$$

where ^{8}B is produced through

$${}^7\mathrm{Be} + \mathrm{H} \rightarrow {}^8\mathrm{B} + \gamma \quad (0.016\%). \quad (8)$$

The pp neutrinos are, by far, dominant in intensity while lowest in energy ($\leq$420 keV). The flux at the Earth is $\approx 6\times10^{10}/\mathrm{cm}^2\mathrm{s}$ and it depends rather insensi-

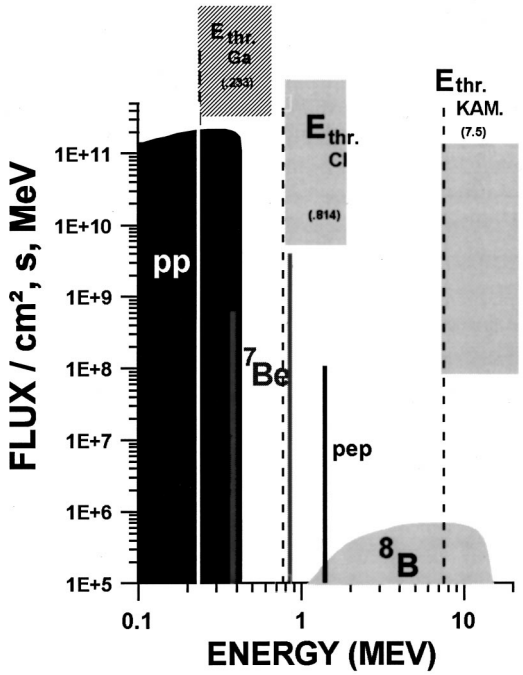

FIG. 1. The solar neutrino spectrum expected according to the standard solar model, SSM (Bahcall *et al.*, 1998a). The energy thresholds for the major solar neutrino detectors are indicated by the vertical dashed lines.

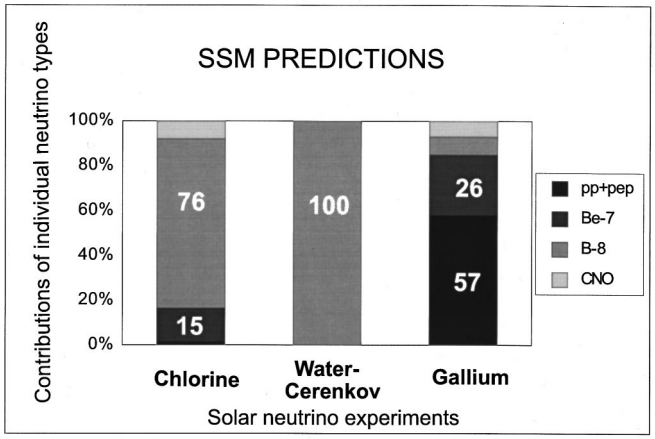

FIG. 2. Relative proportions of the contributions from the various neutrino sources towards the total expected signal (set=100%) in the major types of solar neutrino experiments. The solar model data input is as in Fig. 1. The small contribution from PPI in the chlorine experiment is due to 1.44 MeV pep neutrinos, see Eq. (3). For errors (not shown), see Secs. IV.A and IV.D.

tively on the particulars of any solar model variations. This flux, in fact, follows from the solar luminosity and Eq. (1).

For the case of the ^{7}Be neutrinos, the flux at the Earth is predicted to be $\approx 5\times10^9/\mathrm{cm}^2\,\mathrm{s}$ and varies approximately with T_c^{10}, where T_c is the central solar temperature (Bahcall and Ulmer, 1996). Their energy is intermediate, and they are mono-energetic ("line sources" at 0.86 MeV and at 0.38 MeV).

The ^{8}B neutrinos are rare ($\approx 5\times10^6/\mathrm{cm}^2\,\mathrm{s}$), are model dependent ($\propto T_c^{18}$), and have a continuous energy spectrum up to ≈14 MeV. Suppression of this channel for energy production would have no impact on the solar luminosity.

A further category of neutrinos is the "CNO" neutrinos, which stem from positron decay of ^{13}N, ^{15}O, and ^{17}F, produced in the CNO cycle. The latter is of minor importance for the Sun, and so are these "CNO neutrinos" in the context of the present article.

The neutrino spectrum that results from the SSM is shown in Fig. 1, together with the energy thresholds of the available experiments. For explicit flux tables from the various model calculations see Table 3 in Castellani *et al.* (1997) and Bahcall *et al.* (1998a). The uncertainties of the flux predictions are estimated to be about ±1% for pp neutrinos, ±10% for ^{7}Be neutrinos, and ±20% for ^{8}B neutrinos (see, e.g., Bahcall *et al.*, 1998a). These errors reflect primarily the different degrees of model dependence for the different neutrino branches. The influence of the errors on cross section values and branching ratios is secondary. During the last few years, the determinations of the cross sections (S factors) for the solar fusion reactions have become more accurate, mainly because the laboratory measurements could be extended to lower energies. Because of this, less reliance is needed on extrapolations towards the Gamov-peak energies that are relevant inside the Sun (Junker *et al.*, 1998; see also Castellani *et al.*, 1997; Adelberger *et al.*, 1998).

Folding the neutrino spectrum with the respective detector cross sections yields the expected production rates due to the individual neutrino sources for the various solar neutrino detectors. The resulting spectral sensitivity of the major solar neutrino detectors is shown for comparison in Fig. 2. For each type of experiment, the figure shows the expected relative contributions from the different neutrino branches as a percentage of the total rate. Note that pp neutrinos can be measured only with gallium detectors (except that the expected chlorine detector signal contains a tiny contribution from 1.44 MeV "pep" neutrinos).

B. Neutrino mass mediated propagation phenomena

If some or all neutrino masses are nonzero, flavor oscillations would be a natural consequence (Wolfenstein, 1978). This implies a departure from the standard model of electroweak interactions. In this case, solar neutrinos generated as electron neutrinos ν_e could be converted into ν_μ, ν_τ or into ν_s [neutrinos that are "sterile" under (V-A) interactions due to having the wrong helicity].

Detectors tuned only to ν_e would register a deficit and thus constitute a "disappearance" experiment. Future detectors may eventually be capable of detecting other flavors as well ("appearance" experiment, e.g., SNO see Sec. VI.A). The effective reduction factor, which accounts for the disappearance of ν_e neutrinos along the baseline between the Sun and the detector, depends on

the neutrino mass parameters, the mixing angles, and the neutrino energy. For the case of vacuum oscillations, the oscillation length L is proportional to $E_\nu/\delta m^2$. For the case of $\nu_e \leftrightarrow \nu_\mu$, for example, we have

$$\delta m^2 = |m_{\nu_1}^2 - m_{\nu_2}^2| \quad \text{where} \quad \nu_e = \nu_1 \cos\theta_{12} + \nu_2 \sin\theta_{12},$$
$$\nu_\mu = -\nu_1 \sin\theta_{12} + \nu_2 \cos\theta_{12}. \tag{9}$$

Here, the ν_i are the mass eigenstates with mass m_i, and θ_{ij} is the mixing angle parameter for mass states ν_1 and ν_{12}. Depending on the actual mass and mixing parameters, the respective depression factors can be calculated for the different neutrino energies (or vice versa). Due to the long baseline, mass differences as small as $\delta m^2 \approx 10^{-11}\,(\mathrm{eV}/c^2)^2$ are accessible for study using solar neutrinos. Moreover, even if the vacuum mixing angle is small, very effective flavor conversion can occur through coherent neutrino-electron scattering at high electron-densities ρ_e in the solar interior [Mikheyev-Smirnov-Wolfenstein (MSW) effect, Mikheyev and Smirnov (1986)]. Then, effective mixing, θ_{eff}, becomes maximal at a resonance density $\rho_{e,\mathrm{res}}$, according to

$$\tan\theta_{\mathrm{eff}} = \frac{\sin^2 2\theta_{\mathrm{vac}}}{\cos 2\theta_{\mathrm{vac}} - \cos(L\rho_e)} \quad \text{for} \quad \rho_{e,\mathrm{res}} = 2\theta_{\mathrm{vac}}/L. \tag{10}$$

1. Time variations

MSW conversions are isolated flips rather than true oscillations. Mostly only one flip occurs inside the Sun; another flip may occur when the neutrino beam passes through the Earth. This can cause a partial reconversion into the initial neutrino flavor. The exact mixing parameters and therefore the reduction factors will then depend on the exact density profile traversed within the Earth. This can result in day-night and zenith-angle variations (Maris, 1997).

The time scales of variations in MSW-mediated scenarios are distinct from those encountered for vacuum oscillations. The oscillation length, L, for vacuum oscillation solutions is generally fine-tuned. Small distance changes can be sufficient to bring the conversion factors in or out of resonance. Consequently, the distance variation due to the eccentricity of the Earth's orbit can lead to semiannual time variations for certain $(\delta m^2, \theta_{\mathrm{vac}})$-parameter sets. This is on top of the trivial flux change $\propto r^{-2}$ that causes up to 7% rate change during the year. The latter effect might be used to serve as unambiguous signature for the solar origin of a time series of observations. Until now, statistics have not been sufficient for this proof in any of the operating solar neutrino experiments, but the effect is considered in the conceptions of future experiments like Borexino, and others.

Finally we address the case of oscillation scenarios that involve magnetic interactions of neutrinos with the magnetic fields in the convection zone of the Sun. In this case, time variations could be expected to follow time scales of some years, related to the phase of the 22-year solar cycles (see also Sec. IV.A).

III. DETECTION PRINCIPLES

Two major types of solar neutrino detectors are distinguished: "radiochemical" experiments (based on inverse beta-decay) and "real-time" experiments (e.g., Čerenkov or scintillation detectors).

For the case of radiochemical detectors, one accumulates the product nuclei having atomic mass number A and proton number $(Z+1)$ that are produced in the neutrino capture reaction:

$$^A Z(\nu_e, e^-)^A(Z+1). \tag{11}$$

The product species decay with relatively short half-lives. After exposure of the target to near saturation levels of the product nuclei, the latter are removed from the target by a radiochemical separation. The threshold energy of radiochemical experiments is intrinsically defined by the Q value of the detection reaction.

For the case of real time detectors, the events are recorded as a track or a flash of light that is subsequently registered by photo-multiplier "fly's eye" arrangements that observe the fiducial volume of the detector medium. The energy threshold of real-time detectors (mostly using neutrino-electron scattering) is essentially set by electronic's thresholds. This is governed predominantly by the level of background. The background increases exponentially towards lower energy. So far, this has restricted the use of real-time detectors to the measurement of ^{8}B neutrinos above $\approx$6 MeV. Sub-MeV (pp and ^{7}Be) neutrinos are still accessible only to radiochemical experiments. Concerning ^{7}Be neutrinos, this could change in the year 2001, when Borexino is expected to start operation (see Sec. VI.A).

A. Characteristic features of solar neutrino experiments

Characteristic features of all solar neutrino experiments are as follows:

(i) Large target size (multi-tons).

The characteristic magnitude of solar neutrino signals is mirrored in the unit appropriately defined for the experiments: 1 solar neutrino unit (1 SNU) is a production rate of 1 per 10^{36} target atoms and second. Typical event rates are a few neutrino-induced reactions per day in ten- to thousand-ton detectors.

(ii) Location in underground laboratories shielded from cosmic rays.

In radiochemical experiments, (p,n) reactions on the target nucleus $^A Z$ lead to the same product as a neutrino capture. In a typical surface laboratory, the secondary protons due to cosmic ray nucleons and muons would dominate the creation of product nuclei over and above the production rate caused by solar neutrinos. A reduction of the cosmic ray muon flux by factors of 10^3–10^5 is thus required. This reduction factor corresponds to a necessary shielding overburden of at least a few hundred, up to >1000 meters of rock, such as is achievable either in a mine or in a mountain tunnel. Likewise, in real time experiments, similar shielding re-

quirements arise in order to reduce the muon-induced "trigger rate" to an acceptable level.

(iii) Radiochemical purity of the target to avoid side reactions.

MeV protons that can cause (p,n) reactions are also produced from natural radioactive target impurities (uranium, thorium, and daughter products of their α-decay series). These arise via (α,n) and subsequent (n,p) sequences or from (n,p) reactions due to fast neutrons emitted from the rock walls of the underground lab. Depending on the particular experiment, radiochemical purity of order 10^{-10}–10^{-16} g U or Th per gram of target may be required. This is to keep the production due to side reactions (or the trigger rate in real time experiments) at an acceptable level.

(iv) Sensitive detection devices for single event detection.

The products from inverse beta-decay are themselves radioactive by electron capture. When they decay, the detectable radiation in this process consists of x rays and keV-Auger electrons. Such weakly ionizing low energy radiation is normally detected in low-level gas proportional counters that contain the radioactive species as an admixture to the counting gas. Real time detectors are intrinsically sensitive to individual events.

(v) Rigorous detector background reduction.

In radiochemical experiments, typical decay rates are of order $\leqslant$1/day. Consequently, counter backgrounds must be of order $\leqslant$1/week. This rate poses an ultimate challenge for the art of low-level counting. The major prerequisites for approaching this level are radiochemical purity and counter miniaturization (see Heusser, 1995). Further reduction is achieved by energy and pulse shape analysis using fast electronics (transient digitizer).

Ideally, one would want to measure the full solar neutrino spectrum and separate the contributions from the various neutrino branches (such as pp, ^{7}Be, and ^{8}B neutrinos). Direct differential spectral information can only be obtained from real-time detectors, but their use is still restricted to ^{8}B neutrinos, as mentioned.

B. Detector types

1. Radiochemical detectors

The radiochemical detectors integrate all partial neutrino branches, i, having energies above the threshold. This complicates the interpretation of the recorded production rates, S, which measure the sum

$$S=\Sigma_i\langle\phi_i\sigma_i N_t\rangle, \tag{12}$$

where ϕ_i=neutrino flux, σ_i=cross section, N_t=number of target nuclei. Consequently, the energy threshold, $E_{\rm thr}$, is one of the most important criteria for selecting a detector scheme. Required are $E_{\rm thr}<420$ keV for detection of pp neutrinos, $E_{\rm thr}<862$ keV for ^{7}Be neutrinos, and $E_{\rm thr}<14.1$ MeV for ^{8}B-neutrinos. Further criteria are as follows:

(i) Feasibility of the chemical separation of the few product nuclei from the multi-ton quantities of target element. The best practical approach is to arrange for a scheme in which the reaction product is in a volatile chemical form so that it can be flushed out with a gas stream. The gas extraction yield in this process can be controlled by adding a measurable quantity of inactive or even isotopically labeled carrier to the target and tracing its recovery. This technique is used in two major experiments: (1) The Homestake chlorine experiment (Davis *et al.*, 1968; Davis *et al.*, 1997):

$$^{37}{\rm Cl}(\nu_e,e^-)^{37}{\rm Ar}, \tag{13}$$

in which a helium stream is used to flush out ^{37}Ar together with carrier argon from the perchlorethylene target (C_2Cl_4, an organic liquid: 1,1,2,2-tetra-chloroethylene). (2) The Gallex gallium experiment (Kirsten, 1990; Gallex Collaboration, 1992a):

$$^{71}{\rm Ga}(\nu_e,e^-)^{71}{\rm Ge}, \tag{14}$$

in which volatile germanium tetrachloride ($GeCl_4$) containing the ^{71}Ge is flushed with a nitrogen stream from an aqueous gallium chloride solution. The natural isotopic abundance of ^{71}Ga is 39.9%.

(ii) Value and uncertainty of the expected production rate. Required is the knowledge of the energy-dependent neutrino-capture cross sections for the various neutrino types. Such cross sections for inverse beta decay can be deduced from the ft values resulting from the beta decay characteristics of the product nucleus. However, this applies only to ground state transitions. Excited state contributions to the production rate could cause larger uncertainties. Fortunately, the situation in this respect is under control both for chlorine and for gallium, as discussed in Secs. IV.A and IV.D.1, respectively.

(iii) Availability and affordability of multi-ton quantities of the relevant target isotope at highest radiochemical purity.

2. Real-time detectors

Contrary to radiochemical detectors, which only measure a rate, real-time detectors yield event time, energy, and eventually the direction of individual events. So far, only neutrino-electron scattering,

$$e^-(\nu_x,\nu_x)e^- \tag{15}$$

has been successfully applied to solar neutrino detection, namely in the Kamiokande and Superkamiokande water Čerenkov experiments. Here, the recoil electrons are observed in a forward direction relative to the position of the Sun. This process has also some sensitivity for muon neutrinos. Depending on the energy we have for the ratio of electron-neutrino to muon-neutrino scattering, $\approx 4<\sigma(\nu_e)/\sigma(\nu_\mu)<\approx 7$.

Upcoming and future real time experiments (see Sec. VI) will also exploit more target-specific reaction modes, such as the charged current reactions:

$$^{A}Z(\nu_e,e^-)^{A}(Z+1)^*\rightarrow{}^{A}(Z+1)+\gamma$$
$$(e^-,\ \gamma\ \text{coincidence}) \tag{16}$$

or, in particular for the heavy water "SNO detector" (see Sec. VI.A),

$$d(\nu_e, e^-)\mathrm{p,p} \tag{17}$$

and the neutral-current reaction:

$$^A Z(\nu_x, \nu_x)^A Z^* \rightarrow {}^A Z + \gamma, \tag{18}$$

or, with heavy water,

$$d(\nu_x, \nu_x)\mathrm{p,n}$$

(neutron detection, e.g., via $^{35}\mathrm{Cl}+\mathrm{n}\rightarrow{}^{36}\mathrm{Cl}+\gamma$). (19)

Here the element Z is either part of the detector medium (e.g., deuterium in the SNO experiment or argon in the Icarus liquid argon chamber) or it can be added to the water or to the scintillator in solution.

3. Cryogenic and bolometric detectors

A hope for the future is to benefit from the superior energy resolution of cryogenic and bolometric detectors at low temperature (Booth, 1998). One would measure the energy of recoiling electrons or of recoiling nuclei from coherent neutrino scattering. Small energy deposits lead to phonon excitation of solid granules or crystals in the superconducting state or to increasing temperature in dielectric crystals at very low temperature. A major obstacle on the way to accomplish solar neutrino detectors of this type is the development of practical readout devices for ton-size targets.

4. Geochemical solar neutrino detectors

"Geochemical" experiments rely on the detection of long-lived (or even stable) neutrino capture products that are accumulated in natural minerals in the course of geological time (Kirsten, 1991). This is appealing since it makes it feasible to extract information about the mean neutrino flux in the past millions of years. In practice, however, attempts to exploit this option have been discouraging. One depends on the existence of favorable ore deposits that are deeply shielded and that are low in uranium and thorium.

IV. RESULTS FROM SOLAR NEUTRINO EXPERIMENTS

A. Homestake chlorine detector, based on $^{37}\mathrm{Cl}(\nu_e, e^-)^{37}\mathrm{Ar}$

This classic first solar neutrino detector was set up and operated by Raymond Davis, Jr. in the Homestake gold mine in Lead, South Dakota (Davis *et al.*, 1968). It was the only active solar neutrino experiment for more than 20 years, until 1987. The conception of experimental solar neutrino detection by means of inverse beta-decay reactions was first suggested by Pontecorvo (1946). However, the realization appeared to be utopian: to detect a few atoms out of hundreds of tons of target material seemed impossible. Perhaps the greatest achievement of the Davis experiment is to have overcome the prejudice of seeming impossibility by doing the experiment.

The energy threshold for neutrino capture on ^{37}Cl is 814 keV. Consequently, the detector does not see the most abundant (91%) pp neutrinos (maximum energy 420 keV), but it can detect ^{8}B and ^{7}Be neutrinos from the PPIII and PPII branches, Eqs. (7) and (4), respectively.

Neutrino flux predictions from solar models are converted into expected production rates for the experiment by application of the respective neutrino capture cross sections. Since Davis started to construct his experiment, the theoretical expectation value for the ^{37}Ar production rate has undergone drastic changes, but during the following 30 years it has stabilized at least within a range between 6 and 10 SNU, with a value near 8 SNU being most widely favored (Table I). Most of the production is due to ^{8}B neutrinos, only a minor contribution ($\approx$15%) is expected to come from ^{7}Be neutrinos (see Fig. 2). The cross section for ^{8}B-neutrino capture on ^{37}Cl, 1.14×10^{-42} cm^2 (Aufderheide *et al.*, 1994), is quite reliable since the capture rate is dominated by the transition to the isobaric analogue state near 5 MeV (Bahcall, 1964). Hence, the strengths can be accurately ($\approx$10%) deduced from the ^{37}Ca beta-decay properties. The relatively large uncertainty of the overall production rate is mainly due to the uncertainties of the ^{8}B-flux predictions of the solar models, which differ in the details of treatment and of the input parameters used. Even moderate differences of the central solar temperature deduced from the various models lead to substantial ^{8}B-ν flux changes, $\propto T_c^{18}$. In addition, determinations of the $^7\mathrm{Be}(\mathrm{p},\gamma)^8\mathrm{B}$ cross section yield still variable results (Bogaert *et al.*, 1997).

The most recent standard solar model includes a treatment that accounts for the diffusion of heavy elements (Bahcall *et al.*, 1998a). The latest expected total rate is $(7.7\pm{}^{1.2}_{1.0})$ SNU(1σ). Greater than 90% of the error associated with this number is due to the uncertainty associated with the contribution from ^{8}B neutrinos.

When Davis started his experiment in 1968, there was no way to aim for pp-neutrino detection because of the low threshold needed; gallium was unavailable in large quantities at that time. Instead, 615 tons of perchlorethylene could be acquired at reasonable cost. Low-level counting of ^{37}Ar (electron-capture, half-life 35 d) was well developed from studies of cosmic ray interaction products in freshly fallen meteorites. The 100 000 gallon target contains 133 tons of ^{37}Cl (the natural isotopic abundance of ^{37}Cl is 24.2%). It is exposed in a single tank below 1480 m of rock. At a shielding depth of 4200 meter water equivalent (m.w.e.), the residual muon flux is only $\approx$4 muons/m^2 d. Every few months, the ^{37}Ar is flushed out from the target with helium, collected on a charcoal trap, purified of noninert gases, and admixed to the counting gas of small gas proportional counters (active volume of order 1 cm^3). The Auger peak from ^{37}Ar electron capture is identified at 2.82 keV energy. Since only a few ^{37}Ar atoms are seen to decay per Ar-extraction run, the experiment required the ultimate in refinement of the extraction and counting techniques and in the reduction, recognition, or exclusion of back-

TABLE I. Results from all five solar neutrino experiments compared against the theoretical signal, $S_{\rm th}$. Quoted errors are all 1σ. Experimental errors include systematic errors.

Experiment	HOME-STAKE	KAMIO-KANDE	SUPERKAM-IOKANDE	GALLEX	SAGE
Energy threshold	0.814 MeV	7.5 MeV	7 MeV (E_ν)	0.233 MeV	0.233 MeV
Sample	108 runs	2079 days	708 days	1593 days for 65 runs	52 runs
Period	1970–1994	1987–1995	1996–1998	1991–1997	1990–1997
Reference	Cleveland *et al.* (1997a)	Fukuda *et al.* (1996)	Y. Suzuki, (1999b)	Gallex Collaboration (1999)	Sage Collaboration (1999)
Prediction, $S_{\rm th}$ (Bahcall *et al.*, 1998a)	$7.7^{+1.2}_{-1.0}$ [SNU]	$5.15^{+0.98}_{-0.72}$ [10^6 ^{8}B-ν/cm^2 s]	$5.15^{+0.98}_{-0.72}$ [10^6 ^{8}B-ν/cm^2 s]	129^{+8}_{-6} [SNU]	129^{+8}_{-6} [SNU]
Experimental result, $S_{\rm exp}$	2.56 ± 0.22 [SNU]	2.82 ± 0.38 [10^6 ^{8}B-ν/cm^2 s]	2.42 ± 0.08 [10^6 ^{8}B-ν/cm^2 s]	77.5 ± 8 [SNU]	66.6 ± 8 [SNU]
Observed ratio $R=S_{\rm exp}/S_{\rm th}$	$(33\pm6)\%$	$(55^{+13}_{-11})\%$	$(47^{+9}_{-7})\%$	$(60\pm7)\%$	$(52\pm7)\%$
Reduction factor $R^{-1}=S_{\rm th}/S_{\rm exp}$	3.0	1.8	2.1	1.7	1.9
Deficit (absolute) $\Delta\pm\delta\Delta=S_{\rm th}-S_{\rm exp}$	$5.14^{+1.22}_{-1.02}$ [SNU]	$2.33^{+1.05}_{-0.81}$ [10^6 ^{8}B-ν/cm^2 s]	$2.73^{+0.99}_{-0.73}$ [10^6 ^{8}B-ν/cm^2 s]	$51.5^{+11.2}_{-9.8}$ [SNU]	$62.4^{+11.2}_{-10.1}$, [SNU]
Significance of minimal deficit $\lvert\Delta/\delta\Delta\rvert$	5.0 [σ]	2.9 [σ]	3.7 [σ]	5.3 [σ]	6.2 [σ]

grounds. Rise-time analysis is used to distinguish between slowly rising counter background from gamma ray induced Compton-like extended events and fast, ^{37}Ar decays. The background achieved is <1 count per month.

The Homestake detector has been operating since 1968 with only minor interruptions. Data are reported for the combined 108 runs made between 1970 and 1994 (Cleveland *et al.*, 1997a). In Fig. 3, we display the results obtained since 1970. The result from a single run has little meaning because of the very small number of events observed per run. However, taken together, the data from 20 years of solar neutrino recording have acquired a remarkable significance. The 1σ statistical error is $\approx$6% of the measured signal.

There has been a long history of questioning various aspects of the experiment, yet virtually all suspicions could be disproved by Davis and collaborators in side experiments. Although the ultimate test of exposing the Cl detector to a low-energy neutrino calibration source has not yet been done, consensus has developed that the overall results of the chlorine experiment are reliable.

In judging whether there is a real-time variation among the data (for some time an anticorrelation with the 11-year solar activity cycle had been proposed) one must recognize the statistics of small numbers (the ^{37}Ar production rate is 0.484 ± 0.042 ^{37}Ar atoms/d; see also Sec. IV.B for the absence of such effects in Kamiokande). We should note however that a plausible scenario for a solar cycle correlation has been described [VVO effect, see Voloshin, Vysotsky, and Okun (1986)]. It is related to magneto-coupled neutrino flavor flips into a postulated state that is sterile under (V-A) interactions ("sterile" neutrino, ν_s). This possibility depends on the changing polarity of the strong magnetic fields in the convective zone of the Sun, if neutrinos have a non-

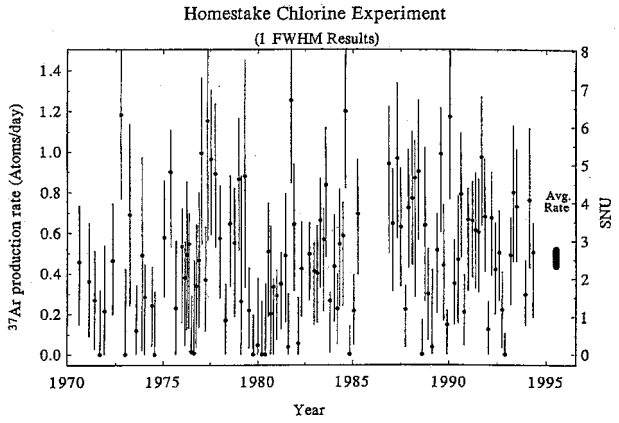

FIG. 3. Results from 108 individual solar neutrino observations made with the Homestake Chlorine detector. The individual error bars are statistical only. The cumulative result shown at the right includes systematic errors. No significant time variation is inherent in the data. Figure from Cleveland *et al.* (1997a).

vanishing magnetic moment. This in turn would imply a nonzero neutrino mass in the standard scenarios.

The overall distribution of the results from the individual Homestake runs is consistent with the assumption of a production rate constant in time and justifies the deduction of a mean value. This result, after subtraction of contributions from side reactions (≈15%, mainly due to residual muons) is (2.56±0.16[stat]±0.15[syst]) SNU or, with errors combined in quadrature, (2.56 ±0.22) SNU(1σ) (Cleveland *et al.*, 1997a).

At a 95% confidence level, the observed rate is ⩽3 SNU, and this has to be compared to the predicted rate, $(7.7^{+1.2}_{-1.0})$ SNU (Bahcall *et al.*, 1998a). The observation is (33±6)% of this expectation (Table I; see also Fig. 7 for illustration and Sec. V.A for the implications of this result).

B. Kamiokande Čerenkov detector, based on $e^-(\nu_x,\nu_x)e^-$

Additional experimental data on solar ^{8}B neutrinos has become available since 1987 from the Kamiokande water Čerenkov detector (Hirata *et al.*, 1990; Fukuda *et al.*, 1996). This detector was originally installed at the Kamioka mine in Japan to search for the decay of the proton. In 1986, it was converted from a "GeV detector" into a "10 MeV detector." This was accomplished by lowering the intrinsic contamination of the water. The long-lived natural radioactivity (U, Th decay series, ^{40}K) was reduced to a level at which it became feasible to observe the neutrino-induced recoil electrons having energies as low as ≈7 MeV. In this way, at least the upper part of the ^{8}B solar neutrino spectrum became accessible. The detector is installed below 2700 m.w.e. of shielding. This is not quite as much as one would ideally wish to have but sufficient to reduce the background from muons and short lived spallation products in the water to an acceptable level. The detector is able to record data on the conic Čerenkov-light emission produced by recoil electrons in the 2142 tons of water. The water pool is lined with a dense network of large photo multiplier tubes (PMT's) and surrounded by a 2-meter wide anticoincidence network that functions on the same principle. The innermost 680 tons were used as the sensitive fiducial volume. The energy and the position of an event are reconstructed by using the number and geometric orientation of the PMT cells hit by the Čerenkov light cone together with the relative event arrival times. The energy resolution in Kamiokande was 22% at 10 MeV; the vertex resolution 1.7 meter; the angular resolution ±28°; and the time resolution 5 ns.

The cross section for ν_e-e^- scattering of solar ^{8}B neutrinos with $E>10$ MeV is $\approx 2\times10^{-45}$ cm^2. The spectrum of the recoil electrons reflects the initial neutrino spectrum in a theoretically well-understood fashion. In the energy range of interest here, the mean energy shift of the recoil electron spectrum relative to the incident neutrino spectrum is about 0.5 MeV. Triggered events are sorted according to the number N_h of PMT's hit per event. For instance, a 10 MeV neutrino yields an average $N_h=22$ in Kamiokande.

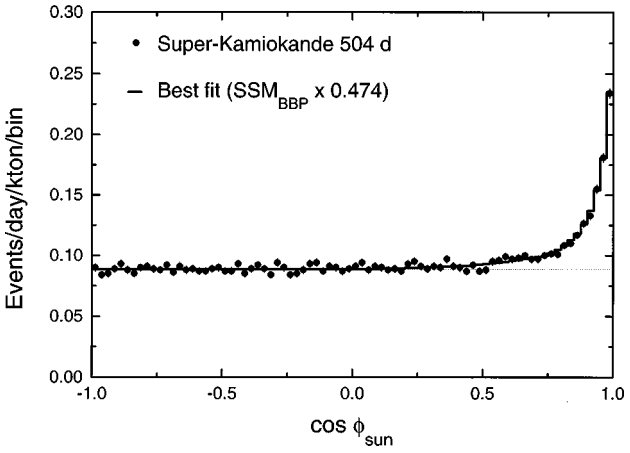

FIG. 4. Distribution of the events remaining with energy >6.5 MeV after all cuts for the first 504 days of Superkamiokande observations. The event rate per day per kiloton is plotted versus $\cos\phi_{\rm sun}$. Here, $\phi_{\rm sun}$ is the angle between the trajectory of the scattered electrons and the direction of the Sun. The total sample contains 8705 events. The solid line compares the data with 47.4% of the expectation value from the standard solar model of Bahcall *et al.* (1998a). Evident is (i) that the signal comes from the direction of the Sun, and (ii) the observed flux from the Sun's direction is only about half of the SSM prediction. The figure refers only to a sub-sample of the full data considered in the text (Y. Suzuki, 1999b; and Table I). Figure after Y. Suzuki (1999a).

In spite of the provisions described above, the task to recognize solar neutrino induced events is formidable and requires extremely good criteria for track recognition and timing. Note that the total trigger rate for the detector was a quite high 150 000/d, while the expected signal surviving all necessary cuts is <1 event/d. The major cuts are based on selecting the energy acceptance window (e.g., $22<N_h<36$); rejecting muon-induced events with the outer anticoincidence counter, and setting the event separation time to >100 μs in order to recognize decay electrons from stopped muons; requiring the vertex to be inside the fiducial volume in order to reject external γ's and neutrons; performing a time analysis to reject 10–15 MeV beta particles from short-lived, muon-induced spallation products on oxygen; and finally, on requiring the event to be produced from the direction of the Sun, to within a 37° cone at a 90% probability for acceptance. After all of these cuts a signal from the Sun's direction is clearly visible. However, it is not nearly as high as predicted from the SSM (see Fig. 4, even though this figure applies actually to Superkamiokande). The mean observed event rate for the solar signal was found to be ≈0.4/d during the 2079 days of Kamiokande observations between January 1987 and February 1995. The ^{8}B-neutrino flux measured by Kamiokande is (2.82±0.19[stat]±0.33[syst])10^6/cm^2 s (Fukuda *et al.*, 1996). This is to be compared to the theoretical flux prediction of $(5.15^{+0.98}_{-0.72})10^6$/cm^2 s (Bahcall *et al.*, 1998a). In summary, only 55% of the expected ^{8}B neutrinos are found. The deficit of 45% is significantly larger than the errors of the flux measurement by Kamiokande (Table I).

An analysis has been made to search for time variations of this flux: (i) over almost a full solar cycle, and (ii) by separation of the day and night data records. The latter is a test for flavor oscillations that are affected by a late neutrino passage through the Earth (see Sec. II.B.1). No statistically significant differences have been found as to this respect in the Kamiokande data.

C. Superkamiokande detector, based on $e^-(\nu_x,\nu_x)e^-$

After 9 years of successful solar neutrino recording, Kamiokande was replaced by the larger and cleaner "Superkamiokande" imaging Čerenkov detector. A 50-kiloton tank with ultrapure water is observed by ≈13 000 PMT's, including those for the outer veto water shield (Suzuki, 1997). The fiducial volume of 22.5 kilotons implies upscaling relative to Kamiokande by a factor of 33; hence, Superkamiokande is the first solar neutrino detector with an event rate of order 10 per day rather than 1 per day. Data taking started in May 1996 with the electron energy threshold, $E_{e\,\mathrm{thr}}$, set at 6.5 MeV (Y. Suzuki, 1999a). This corresponds to a neutrino energy of $E_\nu=7$ MeV. Meanwhile, $E_{e\,\mathrm{thr}}$ has been further reduced to 5.5 MeV ($E_\nu=6$ MeV), (Y. Suzuki, 1999b).

The threshold reduction relative to Kamiokande became possible by the successful background reduction, mostly due to cleaning the water. Energy calibration is done with nickel γ sources and by using an electron beam from a tunable linear accelerator at the water tank.

The results from Superkamiokande confirm and detail the ^{8}B-neutrino deficit observed in Kamiokande and Homestake. At this time, 9530 solar events have already been recorded during the first 708 days of measurements (Y. Suzuki, 1999b). The nature of the signal is illustrated in Fig. 4 for a sub-sample of 504 days. The measured ^{8}B-neutrino flux for the full 708 day sample is $(2.42\pm0.04[\mathrm{stat}]\pm0.07[\mathrm{syst}])10^6/\mathrm{cm}^2\,\mathrm{s}$. This corresponds to $(47\pm1.6)\%$ of the nominal (error-free) expected flux according to Bahcall *et al.* (1998a) (Table I and also Fig. 7, discussed in Sec. V.A). The Superkamiokande result is in reasonable agreement with the respective result from Kamiokande, $(55\pm7)\%$ (see Sec. IV.B, and Table I).

The "high" event rate in Superkamiokande raises hopes that in the future one can deduce interesting fine structures, which were formerly hidden by poor statistics. This concerns eventual deviations from the Fermi-shape of the ^{8}B-neutrino spectrum as well as time variations of the neutrino flux (day/night, zenith angle, winter/summer, solar cycle, and stochastic events, see Sec. II.B.1). Observations of this type would signal neutrino mass mediated flavor changes (see also Sec. V.B).

So far, no significant effects of this type have been found within the experimental uncertainties (Y. Suzuki, 1999a; Y. Suzuki, 1999b). An eventual day/night asymmetry is limited to <6%. Also, the errors are not yet at the level that would be necessary to reveal the expected 7% seasonal rate change that is caused by the eccentricity of the Earth orbit (see Sec. II.B.1). Similarly, no deviations from the Fermi shape of the neutrino spectrum have been observed between 7 and 13 MeV. Some excess near the neutrino end-point energy of 14 MeV is indicated, but this is statistically not yet significant. Evidently, interesting insights can be expected in the future from improved statistics. In particular, crucial information could come from the observation of the shape of a larger part of the ^{8}B spectrum. This would require that the acceptable energy threshold could be reduced further.

D. Gallex gallium chloride detector, based on $^{71}\mathrm{Ga}(\nu_e,e^-)^{71}\mathrm{Ge}$

The Gallex experiment was designed to measure in particular pp neutrinos. At the time of the initial proposal, no experiment other than a radiochemical gallium detector was demonstrably able to achieve this goal, and this is still true today. The reason is the low energy of pp neutrinos, $E_{\max}=420$ keV. The threshold of the $^{71}\mathrm{Ga}(\nu_e,e^-)^{71}\mathrm{Ge}$ reaction is 233 keV. As already mentioned, the measurement of the pp-solar neutrinos is particularly desirable because *only this* neutrino species (the major one) is accurately predictable. It is almost solar model independent and can therefore serve as a "known source" in the extreme long-baseline neutrino oscillation experiment, where the source-detector distance is $\approx1.5\times10^8$ kilometers.

The Gallex detector integrates over all neutrino branches above threshold. According to Eq. (12) the expected theoretical rate, S_{th}, in the standard solar model (Bahcall *et al.*, 1998a) is

$$\begin{aligned} S_{\mathrm{all}}=S_{\mathrm{th}}&=S_{\mathrm{pp}}+S_{^7\mathrm{Be}}+S_{^8\mathrm{B}}+S_{\mathrm{CNO}}\\ &=(73+34+12+10)\ \ \mathrm{SNU}\\ &=129\ \ \mathrm{SNU}, \end{aligned} \tag{20}$$

whereby S_{pp} is almost model independent (scaling with ≈89% of the solar luminosity) and $S_{^7\mathrm{Be}}$ is only slightly model dependent (scaling with ≈11% of the solar luminosity). To the contrary, $S_{^8\mathrm{B}}$ and S_{CNO} are strongly model dependent, the predictions for them are not very accurate. The overall expected rate is $129\pm{}^{8}_{6}\,\mathrm{SNU}(1\sigma)$ (Table I).

The experiment was set up in the Gran Sasso Underground Laboratory of the Istituto Nazionale di Fisica Nucleare (INFN) during 1988–1991 (Kirsten, 1990; Henrich and Ebert, 1992; Kirsten, 1992). It is shielded by 3200 m.w.e. of dolomite rock. The target is 100 tons of 8-molar gallium chloride solution containing 30.3 tons of gallium in a 70-m^3 target tank. The tank is equipped with provisions for a nitrogen purge, and with a central reentrant tube for insertion of either a man-made neutrino source or of a calcium-nitrate neutron monitor. The chemical form of the gallium target was chosen to facilitate the extraction of the product, ^{71}Ge, as volatile germanium chloride ($^{71}\mathrm{GeCl}_4$). It is removed by flushing the target liquid with nitrogen. From there on, small-scale lab bench chemistry takes over. $^{71}\mathrm{GeCl}_4$ is con-

verted into germane, GeH_4 (a homologue of CH_4, methane). The minute neutrino induced activity is registered in miniaturized low-level gas proportional counters. The counting gas is a GeH_4/Xe mixture. A low-level counting spectrometer inside a Faraday cage holds the gas counters and serves as a veto shield for them.

Extremely low counter backgrounds (around 1 count per month) are demanded since typically one has only a few ^{71}Ge decays in a single run. The decays are observed via Auger electron and x-ray emission. Energy and fast pulse shape analysis serve to select the candidate events. Then, the maximum likelihood method is used to partition them into a signal from ^{71}Ge decay and a time constant background.

Data taking started in May 1991. Since that date, runs were performed monthly or so until January 1997. The results were published about annually (Gallex Collaboration, 1992a; Gallex Collaboration, 1993; Gallex Collaboration, 1994; Gallex Collaboration, 1995a; Gallex Collaboration, 1996; Kirsten, 1998; Gallex Collaboration, 1999). These cover a total of 65 runs comprising 1593 net days of exposure between May 1991 and January 1997: 324 days in Gallex I (15 runs), 648 days in Gallex II (24 runs), 353 days in Gallex III (14 runs), and 268 days in Gallex IV (12 runs). The Gallex periods were separated by a scheduled change of the target tanks (after Gallex I) and by two Cr-source exposure periods (between GX II/GX III and GX III/GX IV, respectively; see Sec. IV.D.1).

Counting of a run lasted typically for about 6 months in order to fully characterize the very low background after the decay of ^{71}Ge. The individual results for all 65 Gallex solar runs are shown in Fig. 5. A single run result has little meaning because the error is large (typically only about five ^{71}Ge counts are recorded per solar run). However, the statistics assembled during more than 5 years of data taking allowed, under the assumption of a production rate constant in time, to reduce the statistical error to ≈6 SNU (≈8% of the measured signal). Then, the joint result for Gallex (I+II+III+IV) is $(77.5\pm6.2[\text{stat}]\pm^{4.3}_{4.7}[\text{syst}])$ SNU(1σ) or, in short, (78 ± 8) SNU (Table I). This is ≈60% of the SSM expectation value of 129 SNU (see Fig. 7 for illustration and Sec. V for implications from this result).

As is evident in Fig. 5, the results for the four measuring periods GALLEX I, II, III, and IV show appreciable scatter. They are (83 ± 17) SNU, (76 ± 10) SNU, (54 ± 11) SNU, and (118 ± 18) SNU, respectively. The rate for GALLEX III is 2σ below, that for GALLEX IV 2σ above the mean value of 77.5 SNU. Statistical tests were performed to judge whether this might indicate any time variability of the solar neutrino flux.

Altogether about 320 ^{71}Ge atoms produced by solar neutrinos have actually been seen to decay. The analysis for seasonal correlations revealed no statistically significant effects. The distribution of the 65 single run results fits very well the Monte-Carlo generated distribution of 20 000 single run results for a sample in which the mean production rate and the actual conditions of GALLEX

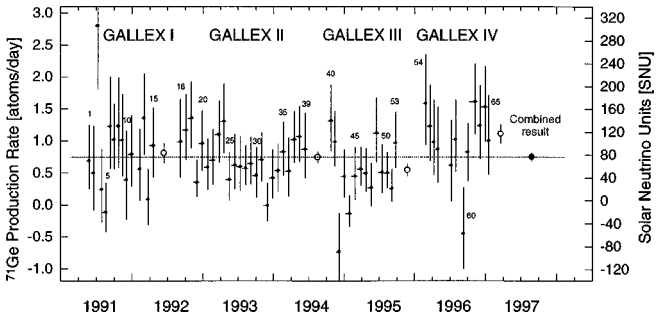

FIG. 5. Results from all 65 individual solar neutrino observations with the Gallex detector. The left-hand scale depicts the measured ^{71}Ge production rate. The right-hand scale indicates the net solar neutrino production rate (SNU) after subtraction of side reaction contributions. Small arabic numerals indicate the sequential solar run number. Error bars (1σ) for individual run results are statistical only. The error bar of the combined result shown at far right, (77.5 ± 8) SNU, includes also the systematic error. Mean values for the four experiment segments, Gallex I, II, III, IV, are also shown. Negative results for individual runs can naturally occur as a result of the maximum likelihood distinction between the signal (exponentially decreasing in time) and a background constant in time. (Imagine, e.g., a situation in which, by chance, the first accepted count occurs after 2–3 half-lives of ^{71}Ge.) Figure from Gallex Collaboration (1999).

I, II, III, and IV are used as input in appropriate proportions. Hence, it is the time sequence of high and low results, not the results themselves, which display larger statistical departures from the mean. The χ^2 test for the results of the four data taking periods yields only a 2.6% probability to be compatible with the mean rate, if the production rate is constant in time. However, instead to speculate on a time-variable neutrino flux, this pattern is associated with statistical fluctuations for a particular choice of binning (Gallex Collaboration, 1999). For example, if the 65 solar runs are grouped into four equal quarters (subsequent run numbers 1–17, 18–33, 34–49, 50–65), the respective probability is 48%. Other groupings tend also to give probabilities >10%, it is just the GALLEX grouping of measuring periods (I–IV) that has a low probability. No significant seasonality can be deduced from the data.

1. Verification of performance and results

The proper function of the Gallex detector was checked in four major ways.

(i) Each run is routinely monitored with ≈1 mg of stable Ge-carrier isotope. The recovery of this carrier is determined by atomic absorption spectroscopy (AAS). Results are regularly >97%. Here the scale is $O(10^{19})$ Ge atoms in 10^{30} target atoms (Henrich *et al.*, 1997).

(ii) In addition to the solar runs, frequent blank runs were performed in order to verify the absence of any target-related artifacts. These blanks are in every respect identical to solar runs except that the exposure time is reduced to one day, the minimum time required to mimic a real run. The result from all 36 blank runs,

after correction for side reactions and short solar exposure, is (-5 ± 5) SNU(1σ), consistent with a null result (Kirsten, 1998).

(iii) In a major experimental effort, sub-MeV neutrino capture in gallium was directly measured by exposing the Gallex detector to well calibrated strong ^{51}Cr-neutrino sources. ^{51}Cr is produced by neutron activation of ^{50}Cr and emits mono-energetic neutrinos:

$$^{50}\mathrm{Cr(n,\gamma)}\,^{51}\mathrm{Cr}, \quad e^- + {}^{51}\mathrm{Cr} \rightarrow {}^{51}\mathrm{V} + \nu,$$
$$\text{electron capture}, \quad T_{1/2} = 27.7 \text{ d}. \tag{21}$$

The natural abundance of ^{50}Cr is 4.35%. The principal neutrino energy is 751 keV (mono-energetic). The sources were produced in the Siloe reactor in Grenoble by repeated neutron irradiation of 36 kg of chromium that was isotopically enriched in ^{50}Cr (38%) (Cribier *et al.*, 1996). Two times the Gallex target was exposed to ^{51}Cr-neutrino sources. Their strength was (1.71 ± 0.03) MCi and $(1.87\pm^{0.09}_{0.06})$ MCi, respectively. The Ge production during these exposures was monitored in altogether 18 ^{71}Ge-extraction runs. The scale of the Cr-source experiments is O(10^2) ^{71}Ge atoms in 10^{30} target atoms, the precision is of the order of ≈10%. The experiments gave an overall response of (95 ± 8) percent (1σ) of the result expected for a cross section of $\sigma_{71} = (58.1\pm^{2.1}_{1.6})10^{-46}$ cm^2, or (100 ± 8)% for $\sigma_{71} = (55.2\pm1.3)10^{-46}$ cm^2; see below, and Bahcall (1997). In any case, the result is compatible with perfect detector response within 1σ (Gallex Collaboration, 1995b; Gallex Collaboration, 1998a). This is particularly relevant because the ^{51}Cr neutrinos are in every respect very similar to ^{7}Be neutrinos from the Sun and it is primarily this branch that is suspected to be missing (see Sec. V.A).

(iv) In a series of ^{71}As-spiking experiments, ^{71}Ge was produced *in situ* by beta decay of ^{71}As (half-life 2.72 d). Here the scale is O(10^4) ^{71}Ge atoms in 10^{30} target atoms, in order to achieve a precision of ≈1%. Therefore, because of the contamination risk, this experiment could be done only after the last solar run was completed. The ^{71}As experiments were performed under variable conditions of extraction and carrier addition, including a carrier-free run. The detector response was perfect in all cases: (100 ± 1)% (Gallex Collaboration, 1998b; Kirsten, 1998).

Given the assurance of an experimental recovery of (100 ± 1)% in Gallex from the As experiments, the result of the Cr-source experiment can be used to determine the effective cross section. This allows one to restrict the contribution of the 175 keV and 500 keV excited states to the neutrino capture cross section on ^{71}Ga. The experimentally determined total cross section is $(55.1\pm4.8)10^{-46}$ cm$^2(1\sigma)$. Using $\sigma_{71} = (55.2\pm1.3)10^{-46}$ cm^2 for the ground state transition, it follows that the excited state contribution is <10% of the total at the 1σ level, in very good agreement with the theoretical estimate, $(5\pm\frac{4}{3})$% of the total (Bahcall, 1997).

In summary, the outcome of all Gallex performance tests is positive. This justifies the conclusion that there are no significant experimental artifacts or unknown errors in Gallex that are anywhere near the ≈40% deficit of the observed solar neutrino signal.

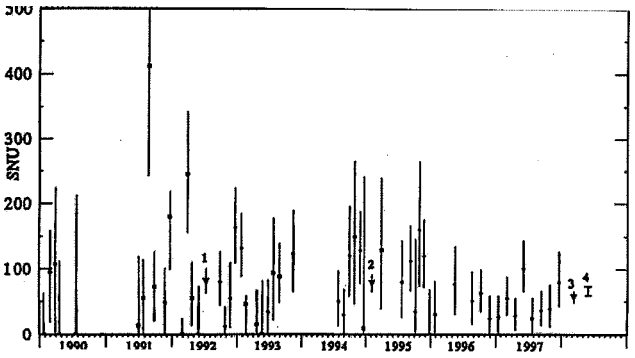

FIG. 6. Results of individual solar neutrino observations with the Sage detector. Group results for Sage I, Sage II, and Sage III are marked "1," "2," "3." The grand total result is marked "4." Figure from Sage Collaboration (1999).

E. Sage gallium metal detector, based on ^{71}Ga$(\nu_e, e^-)^{71}$Ge

Another gallium-germanium experiment was carried out since 1990 by the Sage Collaboration in the INR underground laboratory in the Baksan Valley, Caucasus, at a shielding depth of ≈4700 m.w.e. (Sage Collaboration, 1991a; Sage Collaboration, 1997a). Here the gallium is used in metallic from (it is liquid above 30 centigrade). Germanium is separated by mixing the gallium with an acidic (HCl) and oxidizing (H_2O_2) solution in teflon-lined reaction vessels that are equipped for heavy stirring. Success of the process depends on the formation of a fine emulsion. Once a Ge atom gets in contact with the acidic phase, it leaves the gallium droplet. The experiments have been done with somewhat variable amounts of gallium, up to 57 tons, contained in eight vessels. After the Ge is in the acidic solution, the further chemical and counting procedures are principally similar to those described above for Gallex. An advantage claimed for the Sage process is to have potentially less side reactions within a target that contains fewer protons (free hydrogen atoms) than the aqueous solution used in Gallex. On the other hand, with some worry over potential withholding mechanisms, the processes that occur in a heterogeneous two-phase emulsion are theoretically much less understood than the classical ion chemistry of aqueous solutions. Also, the logistic and technical requirements for an extraction run with metallic gallium in eight vessels are more elaborate. In addition, the need to add in every run substantial quantities of new chemicals aggravates the control of the radiopurity of the target.

Figure 6 depicts the individual run results obtained by Sage between January 1990 and December 1997. About 60 solar runs were performed in this period, but not all of them have been included in the determination of the published results. The latter contain changing sub-sets of runs for certain time periods (Sage Collaboration, 1991a; Sage Collaboration, 1991b; Sage Collaboration, 1994a; Sage Collaboration, 1994b; Sage Collaboration, 1997a). The most recent compilation distinguishes Sage I (14

runs, 1/1990–5/1992, with a gap from 6/1990–6/1991), Sage II (18 runs, 9/1992–12/1994, with a gap from 10/93–7/1994), and Sage III (20 runs, 3/1995–12/1997, with some short gaps in 1995 and 1996) (Sage Collaboration, 1999). The results are (81 ± 20) SNU, (78 ± 13) SNU, and (57 ± 9) SNU, respectively. The overall result for 52 runs is $(66.6\pm^{6.8}_{7.1}[\text{stat}]\pm^{3.8}_{4.0}[\text{syst}])$ SNU(1σ) or, in short, (67 ± 8) SNU, corresponding to 52% of expectation (Table I). The analysis for seasonal correlation reveals no statistically significant effects. The same is true for a comparison of individual run results from Sage and Gallex that are taken at the same time.

In view of the distinct chemical procedure applied, it is important to note that Sage has also performed a successful ^{51}Cr neutrino source experiment (Sage Collaboration, 1996; Sage Collaboration, 1997b). Due to the higher density of gallium metal, less source strength or target mass is required to produce the same number of ^{71}Ge atoms as when gallium chloride solution is used. The Sage source had a strength of (517 ± 6) kCi and was used to irradiate 13.12 t of gallium in a single reaction vessel. The experimental result expressed as a cross section (see Sec. IV.D.1) is $\sigma=(55.2\pm6.6)10^{-46}$ cm$^2(1\sigma)$ (Sage Collaboration, 1999). This is consistent with full response of the Sage detector, demonstrating reliability.

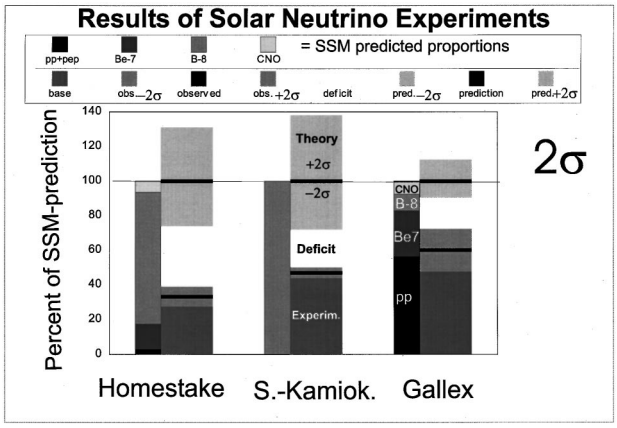

FIG. 7. Major results from the Homestake, Superkamiokande, and Gallex solar neutrino experiments. The SSM expectation values according to Bahcall *et al.* (1998a) are set=100%. Also shown are the $\pm2\sigma$ uncertainties individually for experiments and predictions (95% C.L.). Observed are (33 ± 6)% for Homestake, (47 ± 3)% for Superkamiokande, and (60 ± 12)% for Gallex (2σ, experimental errors only). Sources of data are as described in Sec. IV and summarized in Table I. The spectral composition of the expected signal according to the SSM (Fig. 2) is recalled for the individual experiments in the columns displayed on the left of the major data bars. Statistically significant neutrino deficits (i.e., shortages of the measured neutrino capture rates relative to the predictions) are evident in all cases.

V. IMPLICATIONS

The major results from the experiments described in Sec. IV are compiled in Table I and compared to the expected values based on the SSM. The last line of the table gives the magnitude of the absolute deficit,

$$\Delta=S_{\text{th}}-S_{\text{exp}} \tag{22}$$

expressed in units of the -1σ error, $|-\delta\Delta|$, obtained by quadratic addition of the errors $+\delta S_{\text{exp}}$ and $-\delta S_{\text{th}}$. This allows one to examine and to judge the significance of the minimal absolute deficit.

Here, S_{th} is the theoretical SSM-expectation value according to Bahcall *et al.* (1998a), S_{exp} is the signal measured experimentally. The unit used for S_x is a production rate in SNU for radiochemical experiments and an absolute ^{8}B-neutrino flux in 10^6/cm^2 s for Kamiokande and Superkamiokande.

We note from the table that (1) All solar neutrino experiments observe a signal above zero, (2) all solar neutrino experiments observe fewer neutrinos than predicted from stellar theory, and (3) the reduction factor $R^{-1}=S_{\text{th}}/S_{\text{exp}}$ is ≈3 for Homestake and ≈2 for the other four experiments.

The reliability of the experimental results and their quoted errors has been discussed in Sec. IV. To take the uncertainties of the theoretical model predictions at face value implies that all solar physics processes and input data are considered to be well known and that the quoted spread also covers the range of results obtained for standard solar models by the various authors. While this is generally the case and supported in particular by the recent helioseismological observations (see, e.g., Paterno, 1997), some of the input data (cross sections, opacities) still have appreciable errors. This is considered in the evaluation of δS_{SSM}, whereby individual input errors are added in quadrature [see Bahcall *et al.* (1998a) for a recent discussion of the reliability of SSM predictions].

To illustrate our discussion further, we show in Fig. 7 by proxy the results for Homestake, Superkamiokande, and Gallex. In this graph, the expectation value S_{th} is set equal to 100%. The relative errors $\delta S_{\text{exp}}/S_{\text{exp}}$ and $\delta S_{\text{th}}/S_{\text{th}}$ are shown individually at the $\pm2\sigma$ level, such that missing overlap assures a significant deficit with >95% confidence.

Experimental 2σ errors are ≈7% for Superkamiokande and of the order of 20% for the other four experiments. The 2σ error for the prediction is ≈12% for gallium and of the order of 35% for the other experiments. With error propagation in quadrature for the experimental result and for the prediction, the 2σ uncertainties for the observed absolute deficit, Δ, range from 30% to 70% of that deficit. In other words, even in considering the minimal case, deficits survive at $\geqslant$95% C.L. Expressed in units of the uncertainty, $\sigma=-\delta\Delta$, the absolute deficits are $\Delta\geqslant2.9\sigma$ for Kamiokande and Superkamiokande; $\Delta\geqslant5\sigma$ for the chlorine experiment; and $\Delta\geqslant5.3\sigma$ for the gallium experiments (Table I).

A. Solar neutrino problems

Until 1987, Homestake was the only active solar neutrino detector. The lack of 2/3 of the expected rate in this experiment is known as the "solar neutrino prob-

lem'' since the early 1970's. As much as 76% of the expected signal in the chlorine experiment is due to ^{8}B neutrinos, while ^{7}Be neutrinos contribute 15% (see Fig. 2). Therefore, the deficit was naturally assigned to a ^{8}B-flux reduction. Whether ^{7}Be is also affected could not be decided from the data. It became apparent that the initial problem could in principle be fixed by nonstandard solar models if they were tailored to reduce the central core temperature as needed (by about 5%, from 15.6 to 14.8 million K) or even in standard models by changing the $^7\mathrm{Be}(p,\gamma)\,^8\mathrm{B}$ cross section, σ_{17}, and others (σ_{33},σ_{34}), as well as by changing coupled input parameters such as opacities or initial element abundances (Bahcall, 1989). Fine tuning or (educated) departures from the SSM such as, e.g., He diffusion, heavy element diffusion, rotational mixing, plasma effects, and screening modifications, could in principle all contribute without getting in conflict with the strong constraint provided by the luminosity of the Sun. Many of those models could not be ruled out. Simply put, the prediction from solar physics for the absolute neutrino flux from the tenuous (10^{-4}) PPIII(^{8}B) branch was (and still is) not precise enough to provoke fundamental conclusions from the initial solar neutrino problem alone (see, e.g., the review by Castellani *et al.*, 1997).

At last, in 1990, new evidence from Kamiokande was added, stating that only ≈50% of the ^{8}B neutrinos arrive on Earth. If this is translated into an expectation value for the ^{8}B-induced rate in Homestake, the result is $\approx(3\pm0.5)$ SNU. The measured total rate, (2.56 ± 0.22) SNU, is just compatible with this, but if one takes into account that an additional 1.1 SNU are expected from ^{7}Be neutrinos (and 0.7 SNU from CNO and pep neutrinos), a conflict arose that was later coined the ''second solar neutrino problem'' (Bahcall and Bethe, 1990). Even if all neutrino branches would be subject to the same (50%) reduction, the rate for the chlorine detector should be ≈3.8 SNU, rather than ≈2.6 SNU, as measured.

The second solar neutrino problem persists with modern Superkamiokande data, where the experimental error ($\pm3.3\%$, 1σ) is already much smaller than for the results from 9 years of Kamiokande recordings. Respectively, the updated expectation value for the chlorine detector, assuming equal suppression for all neutrino branches, is 3.62 ± 0.15 SNU. The 1σ error of the theoretical predictions is still of the order $\pm20\%$, but it is not included for the present argument since it affects the Homestake and Kamiokande experiments largely in the same way. To explain the situation after Kamiokande, it was no longer sufficient just to lower the central temperature of the Sun, by whatever means. Instead, a suppression mechanism was indicated that is more effective for ^{7}Be neutrinos than for ^{8}B neutrinos. More precisely, suppression should be enhanced for neutrinos in the energy range 0.8–7.5 MeV, as defined by the condition E_{thr} (chlorine) $<E_\nu<E_{\mathrm{thr}}$ (Kamiokande). This was a strong hint for neutrino oscillations to be involved. To check on this possibility, it was absolutely necessary to get data from an experiment in which the production rate is not dominated by the tenuous ^{8}B neutrinos but by pp and ^{7}Be neutrinos, that is, a gallium experiment (see Fig. 2).

The expected rate for Gallex (or Sage) is dominated by 73 SNU for pp (and pep) neutrinos; that is, they comprise 57% of the total, which is $129\pm^8_6$ SNU (Bahcall *et al.*, 1998a). The second largest contribution (34 SNU) is from ^{7}Be neutrinos. ^{8}B neutrinos are not distinct in the Ga signal; their theoretically expected contribution is only 9% [see Eq. (20)]. Contrary to PPIII (^{8}B), the PPII (^{7}Be) branch is large and robust. Not many possibilities exist to significally affect it by model or input changes. Still, the Gallex result, (78 ± 8) SNU, is only ≈60% of what is expected. The ^{8}B neutrinos present according to Superkamiokande account for 6 SNU. This leaves 72 SNU for pp and ^{7}Be neutrinos, about as much as required for pp neutrinos alone. Hence, there is no room for ^{7}Be neutrinos in the signal, in spite of the fact that ^{7}Be must be present in the Sun in order to account for the ^{8}B flux that has actually been observed in Superkamiokande. This is because ^{7}Be is the precursor of ^{8}B, Eq. (8), and the formation of ^{7}Be has weaker temperature dependence than the formation of ^{8}B. This contradiction constitutes the ''third solar neutrino problem,'' the case of the missing ^{7}Be neutrinos (Gallex Collaboration, 1992b; Bahcall, 1994; Shi *et al.*, 1994; Kirsten, 1995). It cannot be reconciled with solar physics because ≈11% of the solar luminosity are contributed by the PPII cycle. The ^{7}Be-neutrino flux prediction is rather robust also for this reason.

Sage was first in announcing gallium data in 1990. Initially they reported a zero-signal as the most probable result and reflected that the absence of pp neutrinos implied a nonzero neutrino mass (Sage, 1990). However, the result was not statistically significant. Gallex announced its first result, $(83\pm19[\mathrm{stat}]\pm8[\mathrm{syst}])$ SNU(1σ), in May 1992, allowing the full presence of pp neutrinos as expected from the solar luminosity (Gallex Collaboration, 1992a). This was the first observation of solar pp neutrinos, since the result required their presence, at least in part. On the other hand, even the full predicted value for the SSM was still within 2σ of the measurement. In the following years, the errors shrunk and the ^{7}Be deficit became significant (Kirsten, 1995; Kirsten, 1996). The Sage and Gallex results approached the same level and are now in good agreement (see Table I). At present, with a 1σ error of ±8 SNU, it is practically inescapable to conclude that there must be ^{7}Be-neutrino disappearance for reasons that are not related to solar physics.

If pp rather than ^{7}Be neutrinos were held responsible for the deficit in the gallium experiments, this would be even stronger evidence for a nonsolar cause because the pp flux is practically fixed by the solar luminosity.

The third and second solar neutrino problems have made the ^{7}Be-neutrino flux the prime suspect for the observed deficits. In this context, it is particularly relevant that the ^{51}Cr-source neutrinos resemble in every respect ^{7}Be neutrinos (energy, branching; Gallex Collaboration, 1998a). Hence, the source experiments have demonstrated the full detection capability of the detec-

tors, especially for the missing species. Then, with both experimental faults and standard solar physics solutions being excluded as possible explanations for the missing neutrinos, neutrino flavor changes remain as the only viable possibility for a consistent explanation of the evidence.

B. Neutrino oscillations

Quantitative analyses for joint solutions of the solar neutrino problems in the frame of neutrino oscillation scenarios have been performed by many authors (e.g., Hata and Langacker, 1994; Hata *et al.*, 1994; Kwong and Rosen, 1994; Berezinsky *et al.*, 1995; Krastev and Petcov, 1996; Bahcall and Krastev, 1997; Hata and Langacker, 1997; Petcov, 1997), with and without including the MSW effect, the VVO effect (Akhmedov *et al.*, 1997), and the option of conversion into right-handed, noninteracting sterile neutrinos. Vacuum oscillations give consistent solutions at very small mass differences, see Eq. (9), and large mixing angles, centered at $\delta m^2 \approx 8\times10^{-11}\,(\mathrm{eV}/c^2)^2$ and $\sin^2(2\theta_{\mathrm{vac}})\approx 0.75$. However, even better fits for all available data are obtained with the MSW effect, for which two consistent solutions exist in the $(\delta m^2, \theta)$ parameter space.

(1) The so-called "nonadiabatic"—or "small angle"—solution, centered at $\delta m^2 \approx 5\times10^{-6}\,(\mathrm{eV}/c^2)^2$ and $\sin^2(2\theta_{\mathrm{sa}})\approx 6\times10^{-3}$ or, $\theta_{\mathrm{sa}}\approx 2.2°$. This solution yields the best fit and is generally favored. For transformations into sterile neutrinos, $\tilde{n}_s$, the fit is particularly good, at $\delta m^2 \approx 4\times10^{-6}\,(\mathrm{eV}/c^2)^2$.

(2) The "large-angle solution" is centered at a δm^2 that is only slightly higher, but it is near maximum mixing: $\delta m^2 \approx 18\times10^{-6}\,(\mathrm{eV}/c^2)^2$, $\sin^2(2\theta_{\mathrm{la}})\approx 0.76$, $\theta_{\mathrm{la}}\approx 30°$. It became disfavored with shrinking errors in Gallex and with the inclusion of the Superkamiokande zenith-angle dependence in the analysis. For ν_e-ν_s transformations, the large-angle solution disappears altogether.

We have followed here the latest analysis of Bahcall *et al.* (1998b). These authors have included, besides all measured rates, also the day/night, zenith-angle, and spectral data from Superkamiokande (see Secs. II.B.1 and IV.C). Their global fit using all these data is shown in Fig. 8. It favors the small-angle MSW solution, quoted above.

However, the solutions for vacuum oscillations are not completely ruled out. They find some support in the shape of the ^{8}B-neutrino spectrum measured by Superkamiokande. A certain excess of events near 14 MeV (Sec. IV.C) and the nonobservation of a suppression expected for the MSW small-angle solution below 6.5 MeV favor vacuum oscillations (Y. Suzuki, 1999b). However, this leads to values for δm^2 that are at least five times larger then what is obtained from fitting the rates observed in all available experiments for vacuum oscillations. A decision between the options of MSW oscillations and vacuum oscillations could be possible once eventual time variations are established with sufficient statistical significance (see Sec. II.B.1). The answer to this question is among the objectives of Borexino (particular sensitivity for day-night variation) and GNO (semiannual variations).

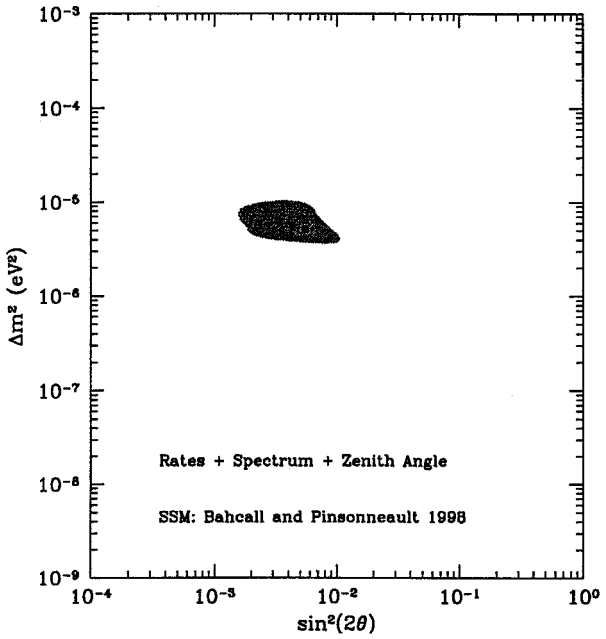

FIG. 8. Neutrino mixing parameter plot. The shaded region is the only allowed MSW solution that is consistent with all solar neutrino data, including the energy spectrum and the zenith angle distribution from Superkamiokande (Superkamiokande Collaboration, 1998). This so-called "small-angle" solution is centered at $\delta m^2 \approx 5\times10^{-6}\,(\mathrm{eV}/c^2)^2$ and $\sin^2(2\theta)\approx 6\times10^{-3}$. Contours are drawn at 99% C.L. Other solutions exist for vacuum oscillations. They are centered at $\delta m^2 \approx 8\times10^{-11}\,(\mathrm{eV}/c^2)^2$ and $\sin^2(2\theta)\approx 0.75$ (not shown). Figure from Bahcall *et al.* (1998b).

C. Neutrino mass and new physics

If it is assured that neutrino oscillations occur, nonstandard neutrinos and "new physics" are a definitive qualitative consequence. On the other hand, a quantitative specification of neutrino masses is less straightforward. The most popular and probably most natural approach is to assume a seesaw neutrino mass mechanism (see, e.g., Mohapatra, 1997) and to assign the dominant mixing of solar neutrinos to $\nu_e \leftrightarrow \nu_\mu$ within a regular lepton-quark mass hierarchy, with $\mathrm{m}(\nu_e) \ll \mathrm{m}(\nu_\mu)$. This leads to a mass estimate for the muon neutrino of $\mathrm{m}(\nu_\mu)\approx 2.2$ meV. Intriguingly, if the observed mixing angle $\theta_{\mathrm{sa}} = 2.2°$ is interpreted as $\theta_{e\mu}$, it agrees well with an estimate based on lepton-quark symmetry considerations according to $\theta_{e\mu} \propto (\mathrm{m}_u/\mathrm{m}_c)^{-0.5}$, where $\mathrm{m}_u, \mathrm{m}_c$ are quark masses. In the same spirit, if lepton-quark family mass scaling according to $\mathrm{m}(\nu_e)/\mathrm{m}(\nu_\mu) \approx m_u^2/m_c^2$ holds, one would obtain, from $\mathrm{m}(\nu_\mu)\approx 2.2$ meV, the electron neutrino mass, $\mathrm{m}(\nu_e)\approx 40$ meV. An estimate for the mass of ν_τ in this pattern comes out at a few eV/c^2,

much above what might be deduced from atmospheric neutrinos (Superkamiokande Collaboration, 1998), see below.

If applicable, the above-described seesaw scenario would lead to some disappointing consequences. Neutrinos would not substantially contribute to hot dark matter. In addition, all attempts to measure the neutrino mass of any flavor in direct experiments would be bound to fail. However, the seesaw mass hierarchy is not the only possibility; other schemes with more or less degenerate neutrino mass relations are also possible (Valle, 1996; Mohapatra, 1997).

1. How compelling is the evidence for new physics from solar neutrinos?

The present situation can be summarized as follows.

The experimental results from five solar neutrino experiments and their error estimates are basically reliable.

Helioseismological observations confirm that the standard solar model is a very good model.

The sizable flux of ^{8}B neutrinos observed is logically incompatible with the near absence of ^{7}B in the Sun as suggested by the paucity if llow energy solar neutrinos (''second and third solar neutrino problems''). This conflict is not traceable to a solar model deficiency resolvable by fine-tuning or changes in the central temperature of the Sun.

Neutrino flavor conversion can consistently account for all solar neutrino data.

No plausible alternatives have yet been suggested.

In conclusion, the evidence is between convincing and overwhelming. However, there is no ''smoking gun.'' The evidence is indirect and based on disappearance. In many respects, the situation is similar to the case of the ν_μ-ν_e anomaly observed for cosmic-ray produced atmospheric neutrinos (Superkamiokande Collaboration, 1998): convincing, yet indirect. The mass difference deduced for these data in terms of MSW oscillations occurring during the neutrino passage through the Earth is $\delta m^2 \approx 5\times10^{-3}\,(\mathrm{eV}/c^2)^2$ (Kajita, 1999), much larger than for the solar neutrino solution, $\delta m^2 \approx 5\times10^{-6}\,(\mathrm{eV}/c^2)^2$. It is consistently explained as result of ν_μ-ν_τ oscillations with nearly maximal mixing, leading to $m(\nu_\tau) \approx 50\,\mathrm{meV}$. Both pieces of evidence indicate the same phenomenon, neutrino oscillations. Consequently, the ''solar'' evidence and the ''atmospheric'' evidence tend to support each other and increase the probability that their interpretation reflects the truth. Continued efforts are needed for the direct proof of neutrino mass. Solar neutrino physics remains an active field.

VI. OUTLOOK

A. Near future

The years 1998–2002 will be a rather active period for solar neutrino exploration. The presently *running* experiments will continue to operate or even become upgraded. In addition, about five *new* detectors will go into operation. Each of them has at least one new specific quality (see, e.g., Kirsten, 1999a).

GNO (Gallium Neutrino Observatory) is the follow-up project of Gallex at Gran Sasso (Bellotti, 1997).

A nonphysical ''zero-cross section'' solar model can define an absolute minimum neutrino flux by setting *ad hoc* and against better knowledge all cross sections for PPII, PPIII, and for the CNO cycle to zero. The only requirement is to sustain the solar luminosity. For this one expects 73 SNU from PPI plus some extra 7 SNU in order to compensate with PPI for the luminosity that is lost in turning off the other branches. Hence, a minimum requirement is ≈80 SNU (Bahcall, 1997). If the CNO neutrinos were preserved, the respective minimum for the rate in a gallium experiment would be ≈88 SNU. Suppose the experimental error of Gallex could be further reduced. Then it could become possible to exclude standard (massless) neutrinos without any reference to solar models. This is the major goal for the GNO experiment.

Data taking started in April 1998 (Kirsten, 1999b). Apart from the above motivation, GNO is intended to provide a long time record of low-energy neutrino observations from 1998 onwards. Gallium detectors remain the only way to register pp neutrinos during 1998–2002. Upscaling to 100 tons of gallium is envisioned for a reduction of the total error to ≈4 SNU. This will also allow a close examination of the time constancy of the pp-neutrino flux during a whole solar cycle.

Sage is planned to operate for a long time. The rather unstable general situation in Russia has required heroic efforts to keep the experiment running.

Chlorine at Homestake has by far the longest continuous solar neutrino flux record and will continue to take data after the present interruption. One envisioned modification is to collect ^{37}Ar produced at day and at night separately. This is to look for the MSW flavor reconversion of neutrinos that penetrate the Earth before they reach the detector.

Superkamiokande will continue to study daily, seasonal, and overall variations of the ^{8}B-neutrino flux. A statistically significant Kurie plot of the ^{8}B-neutrino spectrum should be obtained. This could become a definite test even of the small-angle MSW solution of the solar neutrino problem.

Iodine at Homestake [$^{127}\mathrm{I}(\nu_e,e^-)^{127}\mathrm{Xe}$] started test runs in 1997 with the first 100 tons of iodine (Cleveland *et al.*, 1997b). In many respects, this radiochemical experiment resembles the Chlorine experiment. It has a much higher, but not well-known production rate and benefits from an EC-γ coincidence in the ^{127}Xe decay ($T = 36.4\,\mathrm{d}$). From the beginning, the experiment has been operating in the alternating day/night extraction mode.

SNO (Sudbury Neutrino Observatory) is a 1-kiloton heavy water (D_2O) real-time Čerenkov detector for ^{8}B neutrinos. It is near completion at the Creighton mine in Sudbury, Canada. Assuming that the crucial background problems are in principle solved, data taking is planned to start in 1999 (Meijer-Drees, 1997). The main goal of SNO is to measure not only the spectral shape of ^{8}B

neutrinos above 6.5 MeV in the charged current reaction, Eq. (17), but also the flux ratio $\phi(\nu_e)/\phi(\nu_{\rm all})$ from the neutral current reaction, Eq. (19). This searches for neutrino oscillations not only through disappearance of ν_e but, in effect, also through appearance of ν_μ and ν_τ. It is possible since the disintegration of the deuteron into neutron and proton is independent of neutrino flavor. In this case, the event signature is a 6.25 MeV γ followed by the detection of the neutron, either by capture on ^{35}Cl added or by means of ^{3}He counters (Hime, 1997). In addition, elastic neutrino-electron scattering, Eq. (15), can be observed as in any water Čerenkov detector. With the present installation, the expected event rates are ≈24 per day for the reaction of Eq. (17) and ≈7 per day for the reaction of Eq. (19). The more important data from the neutral current reaction are eagerly awaited for in the year 2000.

BOREXINO is a 100 ton liquid scintillation detector devoted specifically to the detection of ^{7}Be neutrinos through neutrino-electron scattering, Eq. (15). This process is dominated by ν_e since the cross section for the charged current reaction is about 6 times that for neutral current scattering of ν_x. Scintillation detectors have superior light output and better energy resolution compared to Čerenkov detectors. They can operate at much lower energy provided the internal background can be reduced to acceptable levels. This requires the preparation of ultrapure scintillator mixtures in Borexino in order to achieve the extreme radiopurity, especially for ^{14}C and for nuclides from the U, Th-decay series (Hartmann, 1997). Record levels of $<10^{-16}$ g/g uranium and thorium have been achieved in a pilot experiment (CTF=counting test facility). It was shown that backgrounds can be kept at the required level down to a neutrino energy threshold of ≈0.5 MeV, sufficient to detect the flux of the 862 keV ^{7}Be neutrinos (Feilitzsch, 1998; Borexino Collaboration, 1998). This flux would give a strong signal in Borexino if the SSM applies. On the other hand, if the signal were found to be substantially reduced or absent, it would confirm the assignment of the deficits encountered in the gallium experiments to ^{7}Be. The detector is now under construction and planned to go in operation in the year 2001.

Kamland is a project to make use of the old Kamiokande site for a Borexino-like liquid scintillator (A. Suzuki, 1999). The detector will be primarily designed for detection of antineutrinos from a power reactor at ≈150 km distance, operation in this mode might start in 2001. At a later time, low-energy solar neutrino detection is also envisioned, but this would require an additional improvement of radiopurity beyond the present design specification.

Icarus is a fine-grained multipurpose liquid argon drift chamber. It can also be used to detect solar ^{8}B neutrinos above ≈6 MeV. It is sensitive to charged current and neutral current reactions as well as to elastic electron-neutrino scattering. A first 600-ton module is in preparation at Gran Sasso (Rubbia, 1996). The final goal is a 6-kiloton detector. It should register the ^{8}B-neutrino spectrum with high resolution in a relatively short running time.

B. Far future

In the following we describe interesting conceptions and ideas of more or less promising new solar neutrino experiments (see, e.g., Kirsten, 1999a). Intense work of many years has already been invested in some projects; others are at present just good ideas. All of them have in common that at this time one cannot judge whether or when they will eventually become real solar data-taking experiments. Either the physics (mostly background), the technology (large scales), the funding, or all three present unsolved problems. Notwithstanding, some of these proposals may sometime later play an important role. The development of at least one real time pp-neutrino detector is an absolute necessity for the future of solar neutrino spectroscopy.

Radiochemical Lithium experiment (Kopylov, 1997): Early feasibility studies of the system ^{7}Li$(\nu_e,e^-)^7$Be by Davis were aimed at the organic solvent extraction of Be from liquid lithium metal but the unsolved problem was the detection of ^{7}Be. The only detectable radiation emitted from ^{7}Be (half-life 53.3 d) is 43 eV Auger electrons. Now, the Genova group has made remarkable progress with a low temperature microcalorimeter (Galeazzi *et al.*, 1997) and joined with the INR Moscow group to rejuvenate the project. A target as small as 10 tons of lithium metal could be sufficient. With respect to neutrino energy, the expected signal would be rather nonspecific. None of the ν sources above the threshold of 0.86 MeV is clearly dominating the expected SSM production rate of ≈60 SNU.

Radiochemical liquid xenon experiment (Georgadze *et al.*, 1997). The idea is to extract by ion collection techniques ^{131}Cs from ^{131}Xe$(\nu_e,e^-)^{131}$Cs out of 1 kiloton of liquid xenon and to detect it with semiconductors (half-life 9.7 d). ^{7}Be and ^{8}B neutrinos would contribute in about similar quantities. We may remark here that for ^{8}B-neutrino detection, the radiochemical method has been overtaken by present state-of-the-art, real-time detector technology. The counterargument that data from radiochemical detectors (sensitive only to charged current reactions) can serve to distinguish from signals obtained with real-time detectors (which are sensitive to both charge current and neutral current reactions) is specious in view of the size of the experimental errors.

For completeness, we mention here also the status for geochemical experiments in which one attempts to detect long-lived neutrino capture product isotopes in natural minerals by mass spectrometry. Serious but unsuccessful experimental attempts have been reported for ^{81}Br$(\nu_e,e^-)^{81}$Kr*, half-life 2.3×10^5 yrs, use of carnallite containing bromine (Kirsten, 1978), ^{98}Mo$(\nu_e,e^-)^{98}$Tc, half-life, 4.2×10^6 yrs, use of molybdenite ore (Cowan and Haxton, 1982), ^{205}Tl$(\nu_e,e^-)^{205}$Pb, half-life 1.5×10^7 yrs, use of lorandite ($TlAs_2S_2$), Pavicevic (1988). The only still active project of this type is Lorex. Crucial

for this experiment is the question whether better-shielded lorandite ore can be found. The presently available thallium ores are not suitable.

The Hellaz project aims for real time pp-neutrino detection by ν-e scattering in a high pressure, low temperature He-time projection chamber (Tao, 1997). Extreme radiopurity is required for an effective threshold energy as low as 200 keV, and helium is favorable in this respect. Some lab-scale testing has been performed, but the envisioned 10-ton detector (for a rate of $\approx$10 events/d expected from the SSM) is not yet funded.

An approach quite similar to Hellaz but using some advantages of gaseous tetrafluorocarbon instead of helium is investigated in the Super-MuNu project (Broggini, 1998). Such a TPC is primarily developed to determine the magnetic moment of the neutrino but it has also the potential for solar pp-neutrino detection. As in all these ambitious low-threshold experiments, success depends on the practical solution of the background problems in the full-scale detector. Upscaling from small models by more than a factor of five in one step is highly questionable.

The Heron ballistic roton detector aims for pp-neutrino detection in 10 tons of super-fluid helium (Bandler *et al.*, 1995). Excitons from ν-e scattering have long ranges at very low temperature. Their action is transmitted to the surface of the extended liquid helium target. At the surface, rotons evaporate He atoms, which are detected by means of a calorimeter (silicon wafer plus thermistor).

Borexino and Kamland are the only actively pursued liquid scintillation detectors, but quite a few more potential liquid scintillator experiments are considered. Their attraction is the possibility to simultaneously detect (i) charged current reactions, Eq. (16), often with convenient coincidences, (ii) neutral current reactions, Eq. (18), and (iii) neutrino-electron scattering, Eq. (15). The target isotope can be part of the scintillator, like, e.g., hexafluorobenzene in the fluorine experiment (Barabanov *et al.*, 1994):

$$^{19}\mathrm{F}(\nu_e,e^-)^{19}\mathrm{Ne}\ \text{followed by}\ ^{19}\mathrm{Ne}\rightarrow{}^{19}\mathrm{F}+e^+ +\nu_e,\quad \text{half-life 17 s.} \tag{23}$$

The signal would be a delayed coincidence between the electron and the deposition of the decay energy, including the annihilation of the positron.

Another possibility is to dissolve the desired target material in the scintillator. In this way, with some knowledge of chemistry, almost any desired nuclide becomes feasible for investigation. The first such attempt was the indium scintillator experiment [$^{115}\mathrm{In}(\nu_e,e^-)^{115}\mathrm{Sn}^*$, Raghavan (1976)]. The initial hope to benefit from the low threshold of 128 keV to detect pp neutrinos failed because of the natural radioactivity of ^{115}In. However, with the electronic threshold raised to about 600 keV, indium could still make a very good detector for ^{7}Be neutrinos. Notwithstanding, such a project is not presently pursued since Borexino appears to be more advanced for ^{7}Be-neutrino detection.

An attractive experimental scheme with low energy thresholds has the potential to detect even pp neutrinos in real time: LENS (low energy neutrino spectroscopy experiment) proposes to use an ytterbium- or gadolinium-loaded scintillator (Raghavan, 1997) to detect charged current reactions, Eq. (16). Very characteristic beta-gamma coincidence signatures could help to achieve the required background reduction at very low energies. The minimum neutrino energy thresholds are 244 keV for $^{176}\mathrm{Yb}(\nu_e,e^-)^{176}\mathrm{Lu}^*$ and 301 keV for $^{160}\mathrm{Gd}(\nu_e,e^-)^{160}\mathrm{Tb}^*$ for population of the lowest useful excited states of the product nuclides. Additional levels are available for higher neutrino energies. A Lens Collaboration to study the feasibility of the experiment has not yet been formalized but is soon expected to assemble (Lens Collaboration, 1999).

Even solid scintillator crystals such as LiI(Eu) (Chang *et al.*, 1994) or ionization semiconductors such as gallium arsenide crystals (Bowles and Gavrin, 1996) have been considered as remote possibilities for solar neutrino detection.

For the distant future, real technological breakthroughs can also be expected from the development of cryogenic particle and quasiparticle detectors, bolometers, and superconductors. There is a long way to go before such a solar neutrino detector becomes a reality. We refrain here from elaborating on this topic but quote Alessandrello *et al.* (1995) for bolometric detectors using NaBr or CsBr crystals for ^{7}Be-neutrino detection; and Swift *et al.* (1994) for pp neutrino detection using superconducting indium antimonide (InSb) crystals.

In summary, at least some of the experiments discussed in Sec. VI.B seem to be feasible in principle. Whether any one of them will be carried out is an open question. All solar neutrino experiments are expensive and time-consuming projects. Even if all financial and logistical problems can be solved, only after full-scale installation will one know for sure whether the backgrounds in a particular experiment are manageable.

ACKNOWLEDGMENTS

The author thanks J. N. Bahcall and F. X. Hartmann for valuable comments, corrections, and suggestions that helped considerably to improve the manuscript.

LIST OF SYMBOLS

AU	astronomical unit = 149 600 000 km
C.L.	confidence level
CTF	counting test facility in Borexino
d	day
δm^2	$\lvert m^2_{\nu_1} - m^2_{\nu_2}\rvert$ for neutrino mass-eigenstates ν_1, ν_2
EC	electron capture, associated with emission of x rays and Auger electrons
E_{thr}	threshold energy

ϕ_i	neutrino flux of species i
ft value	Fermi function$\times T_{1/2}$ in beta-decay (log)
Gallex	Gallium experiment at LNGS
GNO	Gallium neutrino observatory
GX I, II, III, IV	Measuring periods in Gallex: Gallex I, Gallex II, Gallex III, Gallex IV
Homestake	Chlorine detector at the Homestake mine in Lead, South Dakota
INFN	Istituto Nazionale di Fisica Nucleare, Italy
INR	Academy Institute for Nuclear Research, Moscow
kCi	Kilo-Curie
L	oscillation length
LENS	Project for ''Low energy neutrino spectroscopy''
LNGS	Laboratori Nazionali del Gran Sasso, Italy
m(ν_e)	electron neutrino rest mass
m.w.e.	meters of water equivalent of shielding
MCi	Mega-Curie
MSW effect	Mikheyev-Smirnov-Wolfenstein effect
ν_e, ν_μ, ν_τ	electron, muon, tau neutrino
N_h	number of PMT's hit in a Čerenkov detector
ν_i	neutrino state or type i
ns	nanosecond
pep ν	solar neutrino type, see Eq. (3)
PMT	photo multiplier tube
pp-ν	solar neutrino type, see Eq. (2)
PPI, PPII, PPIII	solar fusion reaction chains
ρ_e	electron density inside the Sun
Sage	Soviet-American gallium experiment
S factor	nuclear reaction cross section stripped of energy dependent part
σ_{ij}	stellar reaction cross-section; i,j are mass numbers of reacting species
SNO	Sudbury neutrino observatory at Sudbury, Canada
SNU	solar neutrino unit, 1 neutrino-induced reaction per 10^{36} atoms and second
SSM	standard solar model
$S_x \pm \delta S_x$	signal due to neutrino-source ''x,'' with error δS_x
t	metric ton
$T_{1/2}$	half-life
T_c	central temperature of the Sun
θ_{ij}	mixing angle for mass- or flavor-neutrino eigenstates i,j
$\theta_{\rm la}$	mixing angle for MSW large-angle solution
$\theta_{\rm sa}$	mixing angle for MSW small-angle solution
$\theta_{\rm vac}$	mixing angle for neutrino states in vacuo
VVO effect	Voloshin-Vysotsky-Okun effect
yrs	years

REFERENCES

Adelberger, E. G., *et al.*, 1998, Rev. Mod. Phys. **70**, 1265.

Akhmedov, E. K., 1997, in *Proceedings Fourth International Solar Neutrino Conference*, edited by W. Hampel (Max-Planck Institut für Kernphysik, Heidelberg, Germany), p. 388.

Alessandrello, A., *et al.*, 1995, Astropart. Phys. **3**, 239.

Aufderheide, M. B., S. D. Bloom, D. A. Resler, and C. D. Goodman, 1994, Phys. Rev. C **49**, 678.

Bahcall, J. N., 1964, Phys. Rev. Lett. **12**, 300.

Bahcall, J. N., 1989, *Neutrino Astrophysics* (Cambridge University Press, New York).

Bahcall, J. N., 1994, Phys. Lett. B **338**, 276.

Bahcall, J. N., 1997, Phys. Rev. C **56**, 3391.

Bahcall, J. N., N. A. Bahcall, and R. K. Ulrich, 1969, Astrophys. J. **156**, 559.

Bahcall, J. N., S. Basu, and M. H. Pinsonneault, 1998a, Phys. Lett. B **433**, 1.

Bahcall, J. N., and H. A. Bethe, 1990, Phys. Rev. Lett. **65**, 2233.

Bahcall, J. N., and P. I. Krastev, 1997, Phys. Rev. C **56**, 2839.

Bahcall, J. N., P. I. Krastev, and A. Y. Smirnov, 1998b, Phys. Rev. D **58**, 096016.

Bahcall, J. N., and M. H. Pinsonneault, 1992, Rev. Mod. Phys. **64**, 885.

Bahcall, J. N., and M. H. Pinsonneault, 1995, Rev. Mod. Phys. **67**, 781.

Bahcall, J. N., M. H. Pinsonneault, S. Basu, and J. Christensen-Daalsgaard, 1997, Phys. Rev. Lett. **78**, 171

Bahcall, J. N., and R. K. Ulrich, 1988, Rev. Mod. Phys. **60**, 297.

Bahcall, J. N., and A. Ulmer, 1996, Phys. Rev. D **53**, 4202.

Bandler, S. R., S. M. Brouer, C. Enss, R. E. Lanou, H. J. Maris, T. More, F. S. Porter, and G. M. Seidel, 1995, Phys. Rev. Lett. **74**, 3169.

Barabanov, I. R., V. Cherehovsky, G. Domogatsky, V. Gurentsov, A. Gurski, A. Kopylov, S. Mikheyev, I. Orekhov, V. Ryasny, and G. Zatsepin, 1994, Nucl. Phys. B (Proc. Suppl.) **35**, 461.

Basu, S., W. Chaplin, J. Christensen-Dalsgaard, Y. Elsworth, G. Isaak, R. New, J. Schou, A. Thompson, and S. Tomczyk, 1997, Mon. Not. R. Astron. Soc. **292**, 243.

Bellotti, E., 1997, in *Proceedings Fourth International Solar Neutrino Conference*, edited by W. Hampel (Max-Planck Institut für Kernphysik, Heidelberg, Germany), p. 173.

Berezinsky, V., G. Fiorentini, and M. Lissia, 1995, Phys. Lett. B **341**, 38.

Bogaert, G., *et al.*, 1997, in *Proceedings Fourth International Solar Neutrino Conference*, edited by W. Hampel (Max-Planck Institut für Kernphysik, Heidelberg, Germany), p. 32.

Booth, N., 1998, Nucl. Phys. B (Proc. Suppl.) **70**, 161.

Borexino Collaboration, 1998, Astropart. Phys. **8**, 141.

Bowles, T., and V. N. Gavrin, 1996, *Seventh International Workshop on Neutrino Telescopes, Venice, Italy*, 1996, edited by M. Baldo-Ceolin (INFN, Istituto Veneto di Scienze, Lettere ed Arti, Venice, Italy), p. 253.

Broggini, C., 1998, Nucl. Phys. B (Proc. Suppl.) **70**, 188.

Castellani, V., S. Degli'Innocenti, G. Fiorentini, M. Lissia, and B. Ricci, 1997, Phys. Rep. **281**, 390.
Chang, C. C., C. Y. Chang, and G. Collins, 1994, Nucl. Phys. B (Proc. Suppl.) **35**, 464.
Cleveland, B. T., T. Daily, R. Davis, J. R. Distel, K. Lande, C. K. Lee, P. S. Wildenhain, and J. Ullman, 1997a, in *Proceedings Fourth International Solar Neutrino Conference*, edited by W. Hampel (Max-Planck Institut für Kernphysik, Heidelberg, Germany), p. 85.
Cleveland, B. T., *et al.*, 1997b, in *Proceedings Fourth International Solar Neutrino Conference*, edited by W. Hampel (Max-Planck Institut für Kernphysik, Heidelberg, Germany), p. 228.
Cowan, G. A., and W. C. Haxton, 1982, Science **216**, 51.
Cribier, M., *et al.*, 1996, Nucl. Instrum. Methods Phys. Res. A **378**, 233.
Dar, A., and G. Shaviv, 1996, Astrophys. J. **468**, 933.
Davis, R., D. S. Harmer, and K. C. Hoffman, 1968, Phys. Rev. Lett. **20**, 1205.
Davis, R., B. T. Cleveland, T. Daily, J. R. Distel, K. Lande, C. K. Lee, P. S. Wildenhain, and J. Ullman, 1997, in *Proceedings Fourth International Solar Neutrino Conference*, edited by W. Hampel (Max-Planck Institut für Kernphysik, Heidelberg, Germany), p. 64.
Feilitzsch, F. v., 1998, Prog. Part. Nucl. Phys. **40**, 123.
Fukuda, Y., *et al.*, 1996, Phys. Rev. Lett. **77**, 1683.
Galeazzi, M., G. Gallinaro, F. Gatti, P. Meunier, S. Vitale, A. Kopylov, V. Petukhov, E. Yanovich, and G. Zatsepin, 1997, Phys. Lett. B **398**, 187.
Gallex Collaboration, P. Anselmann, *et al.*, 1992a, Phys. Lett. B **285**, 376.
Gallex Collaboration, P. Anselmann, *et al.*, 1992b, Phys. Lett. B **285**, 390.
Gallex Collaboration, P. Anselmann, *et al.*, 1993, Phys. Lett. B **314**, 445.
Gallex Collaboration, P. Anselmann, *et al.*, 1994, Phys. Lett. B **327**, 377.
Gallex Collaboration, P. Anselmann, *et al.*, 1995a, Phys. Lett. B **357**, 237.
Gallex Collaboration, P. Anselmann, *et al.*, 1995b, Phys. Lett. B **342**, 440.
Gallex Collaboration, W. Hampel, *et al.*, 1996, Phys. Lett. B **388**, 384.
Gallex Collaboration, W. Hampel, *et al.*, 1998a, Phys. Lett. B **420**, 114.
Gallex Collaboration, W. Hampel, *et al.*, 1998b, Phys. Lett. B **436**, 158.
Gallex Collaboration, W. Hampel, *et al.*, 1999, Phys. Lett. B **447**, 127.
Georgadze, A. S., H. V. Klapdor-Kleingrothaus, H. Päs, and Y. G. Zdesenko, 1997, in *Proceedings Fourth International Solar Neutrino Conference*, edited by W. Hampel (Max-Planck Institut für Kernphysik, Heidelberg, Germany), p. 283.
Hartmann, F. X., 1997, in *Proceedings Fourth International Solar Neutrino Conference*, edited by W. Hampel (Max-Planck Institut für Kernphysik, Heidelberg, Germany), p. 202.
Hata, N., and P. Langacker, 1994, Phys. Rev. D **52**, 420.
Hata, N., S. Bludman, and P. Langacker, 1994, Phys. Rev. D **49**, 3622.
Hata, N., and P. Langacker, 1997, Phys. Rev. D **56**, 6107.
Henrich, E., and K. H. Ebert, 1992, Angew. Chem. Int. Ed. Engl. **31**, 1283.
Henrich, E., R. v. Ammon, and K. H. Ebert, 1997, in *Proceedings Fourth International Solar Neutrino Conference*, edited by W. Hampel (Max-Planck Institut für Kern-physik, Heidelberg, Germany), p. 151.
Heusser, G., 1995, Annu. Rev. Nucl. Part. Sci. **45**, 543.
Hime, A., 1997, in *Proceedings Fourth International Solar Neutrino Conference*, edited by W. Hampel (Max-Planck Institut für Kernphysik, Heidelberg, Germany), p. 218.
Hirata, K. S., *et al.*, 1990, Phys. Rev. Lett. **65**, 1297.
Junker, M., *et al.*, 1998, Phys. Rev. C **57**, 2700.
Kajita, T., 1999, talk for the Superkamiokande Collaboration at Neutrino 98, XVIIIth International Conference on Neutrino Physics and Astrophysics, Takayama, Japan, 1998, to appear in the Proceedings, edited by Y. Suzuki and Y. Totsuka, Nucl. Phys. B (Proc. Suppl.).
Kirsten, T. A., 1978, in *Proceedings Informal Conference on Status and Future of Solar Neutrino Research, Brookhaven*, 1978, edited by G. Friedlander, BNL report 50879, Brookhaven National Laboratory, Vol. 1, p. 305.
Kirsten, T. A., 1990, in *Inside the Sun*, edited by G. Berthomieu and M. Cribier (Kluwer, Netherlands), p. 187.
Kirsten, T. A., 1991, in *Neutrino Physics*, edited by K. Winter (Cambridge University Press, Cambridge), p. 585.
Kirsten, T. A., 1992, in *Particles and Fields '91, Vancouver Meeting*, edited by D. Axen, D. Bryman, and M. Comyn (World Scientific, Singapore), Vol. 2, p. 942.
Kirsten, T. A., 1995, Ann. (N.Y.) Acad. Sci. **759**, 1.
Kirsten, T. A., 1996, Nuovo Cimento C **19**, 821.
Kirsten, T. A., 1998, Prog. Part. Nucl. Phys. **40**, 85.
Kirsten, T. A., 1999a, in *Neutrino Physics*, edited by K. Winter (Cambridge University Press, Cambridge), Second edition (1998).
Kirsten, T. A., 1999b, talk for the Gallex and GNO Collaborations at Neutrino 98, XVIIIth International Conference on Neutrino Physics and Astrophysics, Takayama, Japan, 1998, to appear in the Proceedings, edited by Y. Suzuki and Y. Totsuka in Nucl. Phys. B (Proc. Suppl.).
Kopylov, A. V., 1997, in *Proceedings Fourth International Solar Neutrino Conference*, edited by W. Hampel (Max-Planck Institut für Kernphysik, Heidelberg, Germany), p. 263.
Krastev, P., and S. Petcov, 1996, Phys. Rev. D **53**, 1665.
Kwong, W., and S. Rosen, 1994, Phys. Rev. Lett. **73**, 369.
Lens Collaboration, 1999, letter of Intent, submitted to INFN/LNGS, 1999.
Maris, M., 1997, in *Proceedings Fourth International Solar Neutrino Conference*, edited by W. Hampel (Max-Planck Institut für Kernphysik, Heidelberg, Germany), p. 342.
Meijer-Drees, R., 1997, in *Proceedings Fourth International Solar Neutrino Conference*, edited by W. Hampel (Max-Planck Institut für Kernphysik, Heidelberg, Germany), p. 210.
Mikheyev, S. P., and A. Y. Smirnov, 1986, Nuovo Cimento C **9**, 17.
Mohapatra, R. N., 1997, in *Neutrino 96, Proceedings of the 17th International Conference on Neutrino Physics and Astrophysics, Helsinki, Finland*, 1996, edited by K. Enqvist, K. Huitu, and J. Maalampi (World Scientific, Singapore), p. 290.
Morel, P., J. Provost, and G. Berthomieu, 1997, Astron. Astrophys. **327**, 349.
Paterno, L., 1997, in *Proceedings Fourth International Solar Neutrino Conference*, edited by W. Hampel (Max-Planck Institut für Kernphysik, Heidelberg, Germany), p. 54.

Pavicevic, M. K., 1988, Nucl. Instrum. Methods Phys. Res. A **271**, 287.
Petcov, S. T., 1997, in *Proceedings Fourth International Solar Neutrino Conference*, edited by W. Hampel (Max-Planck Institut für Kernphysik, Heidelberg, Germany), p. 309.
Pontecorvo, B., 1946, Chalk River Report PD 205.
Proffitt, C. R., 1994, Astrophys. J. **425**, 849.
Raghavan, R. S., 1976, Phys. Rev. Lett. **37**, 259.
Raghavan, R. S., 1997, in *Proceedings Fourth International Solar Neutrino Conference*, edited by W. Hampel (Max-Planck Institut für Kernphysik, Heidelberg, Germany), p. 248.
Rubbia, C., 1996, Nucl. Phys. B (Proc. Suppl.) **48**, 172.
Sage Collaboration, V. N. Gavrin, 1990, talk presented at Neutrino 90, XIVth International Conference on Neutrino Physics and Astrophysics, Geneva, Switzerland, 1990.
Sage Collaboration, A. I. Abazov, *et al.*, 1991a, Nucl. Phys. B (Proc. Suppl.) **19**, 84.
Sage Collaboration, A. I. Abazov, *et al.*, 1991b, Phys. Rev. Lett. **67**, 3332.
Sage Collaboration, J. N. Abdurashitov, *et al.*, 1994b, Phys. Lett. B **328**, 234.
Sage Collaboration, J. N. Abdurashitov, *et al.*, 1996, Phys. Rev. Lett. **77**, 4708.
Sage Collaboration, J. N. Abdurashitov, *et al.*, 1997a, in *Proceedings Fourth International Solar Neutrino Conference*, edited by W. Hampel (Max-Planck Institut für Kernphysik, Heidelberg, Germany), p. 109.
Sage Collaboration, J. N. Abdurashitov, *et al.*, 1997b, in *Proceedings Fourth International Solar Neutrino Conference*, edited by W. Hampel (Max-Planck Institut für Kernphysik, Heidelberg, Germany), p. 126.
Sage Collaboration, J. N. Abdurashitov, *et al.*, 1999, talk presented by V. N. Gavrin, in Neutrino 98, Proceedings XVIIIth International Conference on Neutrino Physics and Astrophysics, Takayama, Japan, 1988, edited by Y. Suzuki and Y. Totsuka, to appear in Nucl. Phys. B (Proc. Suppl.).
Sage Collaboration, V. N. Gavrin, *et al.*, 1994a, Nucl. Phys. B (Proc. Suppl.) **35**, 412.
Shi, X., D. Schramm, and D. Dearborn, 1994, Phys. Rev. D **50**, 2414.
Superkamiokande Collaboration, 1998, Phys. Lett. B **433**, 9.
Suzuki, A., 1999, in Neutrino 98, Proceedings XVIIIth International Conference on Neutrino Physics and Astrophysics, Takayama, Japan, 1998, edited by Y. Suzuki and Y. Totsuka, to appear in Nucl. Phys. B (Proc. Suppl.).
Suzuki, Y., 1997, in *Proceedings Fourth International Solar Neutrino Conference*, edited by W. Hampel (Max-Planck Institut für Kernphysik, Heidelberg, Germany), p. 163.
Suzuki, Y., 1999a, in Neutrino 98, Proceedings XVIIIth International Conference on Neutrino Physics and Astrophysics, Takayama, Japan, 1998, edited by Y. Suzuki and Y. Totsuka, to appear in Nucl. Phys. B (Proc. Suppl.).
Suzuki, Y., 1999b, presented at WIN99, International Workshop on Weak Interactions and Neutrinos, 1999, Cape Town, South Africa.
Swift, A. M., D. J. Goldie, N. E. Booth, P. L. Brink, R. J. Gaitskell, A. D. Hahn, and G. L. Salmon, 1994, Nucl. Phys. B (Proc. Suppl.) **35**, 405.
Tao, C., 1997, in *Proceedings Fourth International Solar Neutrino Conference*, edited by W. Hampel (Max-Planck Institut für Kernphysik, Heidelberg, Germany), p. 238.
Turck-Chieze, S., and I. Lopes, 1993, Astrophys. J. **408**, 347.
Valle, J. W., 1996, Nucl. Phys. B (Proc. Suppl.) **48**, 137.
Voloshin, M. B., M. I. Vysotsky, and L. B. Okun, 1986, Sov. Phys. JETP **64**, 446.
Wolfenstein, L., 1978, Phys. Rev. D **17**, 2369.